Taylor & Francis
Taylor & Francis Group

Geografiska Annaler: Series A, Physical Geography

ISSN: 0435-3676 (Print) 1468-0459 (Online) Journal homepage: www.tandfonline.com/journals/tgaa20

Reconstruction of the glacier dynamics and Holocene chronology of retreat of Helagsglaciären in Central Sweden

Anna Kurop & Sven Lukas

To cite this article: Anna Kurop & Sven Lukas (2024) Reconstruction of the glacier dynamics and Holocene chronology of retreat of Helagsglaciären in Central Sweden, Geografiska Annaler: Series A, Physical Geography, 106:3-4, 96-120, DOI: 10.1080/04353676.2025.2521180

To link to this article: https://doi.org/10.1080/04353676.2025.2521180

Published online: 03 Jul 2025.

GEOGRAFISKA ANNALER: SERIES A, PHYSICAL GEOGRAPHY
2024, VOL. 106, NOS. 3–4, 96–120
https://doi.org/10.1080/04353676.2025.2521180

Reconstruction of the glacier dynamics and Holocene chronology of retreat of Helagsglaciären in Central Sweden

Anna Kurop[a,b] and Sven Lukas[a,c]

[a]Department of Geology, Lund University, Lund, Sweden; [b]Biological and Environmental Sciences, University of Stirling, Stirling, United Kingdom; [c]Institute of Earth and Environmental Sciences, University of Freiburg, Freiburg im Breisgau, Germany

ABSTRACT

Despite significant efforts to reconstruct the Holocene glacial history in Scandinavia, evidence of glacier fluctuations in Sweden has mostly been limited to palaeoclimatic proxies, while dating of direct geological evidence from glacier forelands is still rare. This is the first study in Sweden that has attempted to fully reconstruct dynamics, chronology and palaeoclimate of a glacier throughout the Holocene by applying geomorphological mapping, sedimentology, lichenometry and Equilbrium Line Altitude (ELA) calculation on Helagsglaciären, Sweden's southernmost glacier. Helags valley is occupied by extensive glacial and associated sediments of different ages far beyond the current extent of the glacier, indicating earlier prominent advances dated here to 8.5–8.0 ka, around 1.2–1.0 ka and around 1789 CE, which represents the Little Ice Age (LIA) maximum. During the Holocene, the glacier switched from a polythermal regime with frozen bed at the thinning ice margin and parts of the tongue to a fully temperate one. Today, its southern part remains active and temperate, while the northern is probably cold-based. Using calculated ELAs, the climate during the 8.5–8.0 ka event was reconstructed to be cold and wet; slightly colder and drier during the 1.2–1.0 ka advance; and coldest and driest during the LIA. This agrees well with other paleoclimate and glacier fluctuation reconstructions from Scandinavia. In conclusion, this study demonstrates a wealth of information on past glacier dynamics and palaeoclimate that can be reconstructed from current small cirque glaciers in the Swedish Scandinavian Mountains, highlighting the need to study them more extensively.

ARTICLE HISTORY
Received 17 December 2024
Revised 30 May 2025
Accepted 13 June 2025

KEYWORDS
Glacier; lichenometry; palaeoclimate; geomorphology; sedimentology; Equilibrium Line Altitude

1. Introduction

Glaciers are sensitive indicators of climate change and many are reported to have retreated in recent years in response to global warming (IPCC 2023). Knowledge of the consequences of past glacier retreat can provide us with analogues to the modern situations and be used to predict their future development (e.g. Osmaston 2006; Bakke et al. 2010; Lukas and Bradwell 2010; Gjerde et al. 2016). Reconstructions of the extent and behaviour of palaeoglaciers has thus fuelled our understanding of the current consequences of climate change. In Sweden,

CONTACT Anna Kurop anna.kurop@stir.ac.uk Biological and Environmental Sciences, University of Stirling, Stirling FK9 4LA, United Kingdom

considerable effort has been put into constraining the timing and style of retreat of the Scandinavian Ice Sheet (SIS; Svendsen et al. 2004; Krog-Larsen et al. 2009; Krog-Larsen et al. 2012; Hughes et al. 2015; Stroeven et al. 2016) or mass balance and regime of valley glaciers in the northern provinces such as Sarek and around Kebnekaise (e.g. Karlén 1988; Kleman and Stroeven 1997; Carrivick and Brewer 2004; Radić and Hock 2006; Taveirne et al. 2021; Terleth et al. 2022). However, little is known about the chronology and behaviour of cirque glaciers such as Helagsglaciären in the southern part of the Swedish Scandinavian Mountains, despite intensive research on Norwegian glaciers at similar latitudes (e.g. Lie et al. 2004; Matthews and Dresser 2008; Gjerde et al. 2023; Seier et al. 2024). Wastegård (2022) provides a good review of the current state of knowledge of the Holocene glaciation history in Scandinavia. Evidence of glacier fluctuations in Sweden has mostly been limited to palaeoclimatic proxies while dating direct geological evidence from glacier forelands is still rare. This is in stark contrast to Norway where the latter is common practice (e.g. Matthews 2005; Bakke et al. 2010; Gjerde et al. 2016). In particular, little work has been done in the southern Swedish Scandinavian Mountains, or the Helags valley itself, compared to elsewhere (see section 2.2 for more details).

This study aims to contribute to the reconstructions of the Holocene history of glaciers in Scandinavia by investigating Helagsglaciären, Sweden's southernmost glacier. By combining geomorphological mapping, sedimentology, lichenometry and Equilibrium Line Altitude (ELA) calculation, we seek to establish the times when the glacier advanced and retreated, its dynamics and thermal regime at these times, as well as to assess whether these conditions have changed through time. This study also seeks to elucidate the relationship between the glacier's behaviour and climatic factors to be able to answer the broader question on the significance of small cirque glaciers in reconstructing palaeoclimate in currently scantly-glacierized mountain regions.

2. Site description

2.1. Geological and climatic setting

Helagsglaciären is located in the southern Swedish Scandinavian Mountains (Figure 1). It occupies a 1.5 km-wide cirque, the floor of which lies at 1420–1320m above sea level (a.s.l.) and is cut into the eastern side of Helagsfjället (1797m a.s.l.). The Helags valley drains into the Handölan river valley. The mountain is built from resistant paragneiss with some amphibolite, formed ca. 542–488 Myr (SGU 2017) and stands out among relatively wide and flat terrain from which other individual, flat-topped peaks emerge, some also occupied by cirque glaciers (Sylglaciären, Ekorrglaciären and Tempelglaciären). The area is situated well above the local tree line (around 850 m a.s.l.). Mean summer (Jun-Aug) and winter (Dec-Feb) temperatures are about 8 and −6°C respectively, and annual precipitation equals 1300 mm, mostly as rain in the summer season (SMHI 2013). Despite proximity to the North Atlantic coast, most of the moisture is scavenged by the mountains to the west due to orographic effects and increasing continentality, resulting in a well-established west–east precipitation gradient in the Scandinavian Mountains (Barnekow 2000; Rosqvist et al. 2013; Jansen et al. 2016).

2.2. Previous research on Helagsglaciären

Only limited research has been conducted on Helagsglaciären and its deposits. The earliest known study is the general descriptive work of Enqvist (1910) which focused on the elevation of the glacier ice and its margins, measurements of the firnline as well as basic geomorphology of moraines on the glacier's direct foreland. The study was supplied with photographs of Helagsglaciären and its surroundings and a couple of general topographic maps. Enqvist (1910) speculated about the former greater extent of the glacier based on flat-topped, 'wind-eroded' ridges up to 2 km downvalley of the

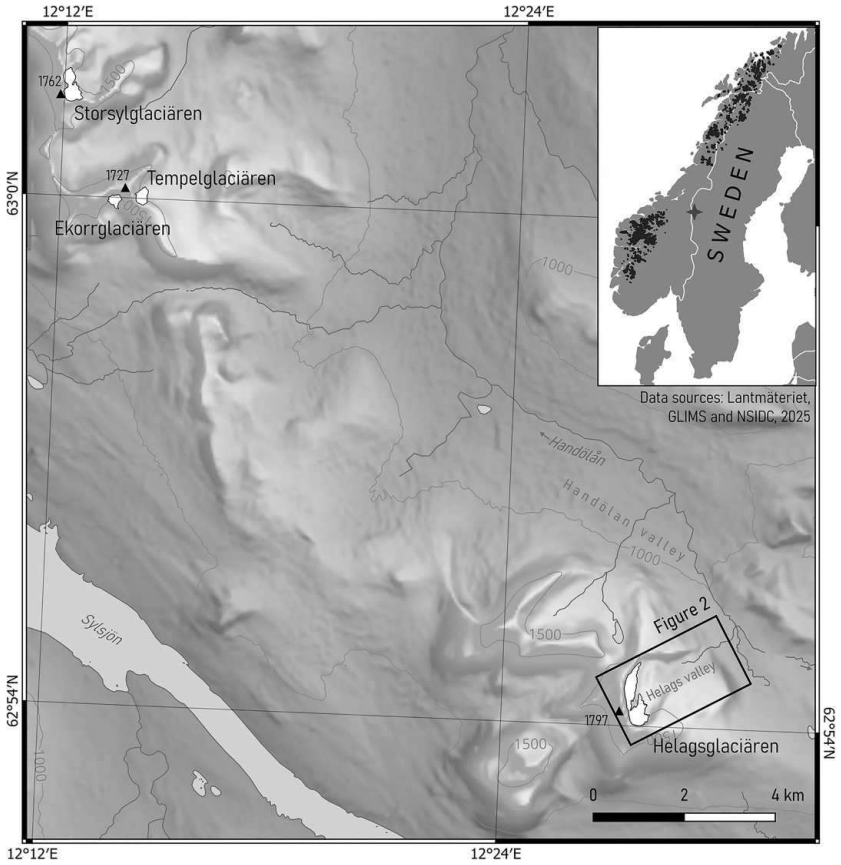

Figure 1. Location and topographical setting of Helagsglaciären. The glacier occupies a cirque cut to the eastern side of Helagsfjället. Neighbouring Sylglaciären, Ekorrglaciären and Tempelglaciären are located to the north-west. The inset shows the current extent of glaciers in Scandinavia.

ice margin at the time. The first identification of the lowermost moraine (1042 m a.s.l.) on the floor of the Handölan valley as the maximum extent of Helagsglaciären was reported by Bergström (1955). Bergström (1955) also attempted to assign the age of deposition to landforms in the Helags valley. The outermost moraine in the valley was referred to as 'lateglacial'. Additionally, deposition around 500 and 1750 CE was suggested for two upvalley moraine complexes (Bergström 1955) distant from each other, though the exact location is unclear.

Lundqvist (1969) mapped the Helags valley using an aerial photograph taken on the 5th Aug 1960. This publication was a description to Jämtland's Quaternary sediment types map created by the Swedish Geological Survey (Sveriges Geologiska Undersökning, SGU), but it also included and reviewed information on local mountains and glaciers. From the photograph, Lundqvist (1969) identified the main latero-frontal moraine ridges from the cirque's headwall to about half the valley's length. That study also noted a considerable retreat of the ice margin since the report by Enqvist (1910).

More recently, Helags valley was mapped as a part of SGU's Quaternary geomorphological mapping programme at a much smaller-scale level, with only some landform identification (Blomdin et al. 2021; SGU 2021). Kullman and Kjällgren (2000) report a radiocarbon date on a fossil pine stump extracted from a little mire in the Helags valley to be 11 160 ± 80 yr BP, later presented as 13 145 cal. yr BP in Öberg and Kullman (2011). A few more birch megafossils were found at Helagsglaciären's foreland, dated to 7790 cal. yr BP, 8620 cal. yr BP and 9520 cal. yr BP (Öberg and Kullman 2011; Kullman and Öberg 2020). Helagsglaciären was mentioned by Rehn (2019) as a glacier that 'should not exist' due to negative mass balance but survives thanks to topoclimatic factors such as protective cirque topography, snowblow and its north-east orientation, and is projected to disappear by 2100 (Tinnerholm 2024).

3. Methods

3.1. Geomorphological mapping

The mapping followed guidelines by Chandler et al. (2018), where remote assessment and preliminary mapping of the terrain is first carried out before validation in the field. For this purpose, LiDAR-based Digital Terrain Model (DTM) sheets with 1.0 ± 0.3 m and 1.0 ± 0.1 m horizontal and vertical resolution, respectively, were downloaded from Lantmäteriet (2022). They were examined in QGIS using a multidirectional hillshade and a slope function, while consulted with underlaid satellite images from Google Satellite (0.5 m) and ESRI World (0.6 m spatial resolution) basemaps. This technique has been widely applied to mapping glacial landforms (e.g. Hughes et al. 2010; Norris et al. 2017).

Fieldwork was carried out from 3–13 August 2022, during which the preliminary geomorphological mapping was validated and refined by field mapping using the QField mobile application geolocation and tracking functions (OPENGIS.ch 2022) with an accuracy of about 2 m.

3.2. Sedimentology

Exposures were dug into moraine ridges by hand and examined using standard approaches (Evans and Benn 2021). Lithofacies analysis was carried out on-site and included description of grain size, lithology, sorting, roundness, colour, structural features and nature of contacts of different lithofacies. Three two-dimensional logs were created using Krüger and Kjær's (1999) recommendations for a graphical key for displaying different features.

3.3. Lichenometry

Lichenometry was first proposed as a relative dating technique by Faegri (1934) and developed by Beschel in the 1950s (e.g. 1955, 1957, 1958). Lichenometry is based on the fact that lichen are long-lived pioneers that start to occupy rock surfaces soon after they stabilize at the Earth's surface. If the growth rate of a lichen is known, the time of the surface exposure can be calculated (see reviews by Bradwell and Armstrong 2007; Benedict 2009; and examples of case studies by Evans et al. 1999; Winkler 2004 and Leigh et al. 2020). However, the growth rate depends on many local factors such as temperature, humidity, slope aspect or rock type and thus is unique to each site, which attracted some criticism of the fundamental principles of this technique (Osborn et al. 2015). Growth rate also varies by lichen species. This facilitates the need to create a lichen diameter-age calibration model by measuring lichen on surfaces of known age before applying lichenometry to a specific area.

Rhizocarpon geographicum in particular has been utilized in most studies as it is widespread in polar and alpine environments (Armstrong 2016). However, the *Rhizocarpon* genus comprises many similar-looking species that make *R. geographicum* particularly difficult to identify without years of expertise. For this reason researchers tend to use the name '*R. geographicum*' as an umbrella term for this plus all other lichen species that can be mistaken for it, most notably *R. alpicola* (Innes 1983; Evans et al. 1999; Armstrong 2016), and therefore admit the risk of misidentification. Despite the uncertainty this introduces (each species has a different growth rate), the approach still yielded satisfactory results (O'Neal 2006). This practise is also adopted here.

Of the many approaches to measure lichen diameters, the one proposed by Evans et al. (1999) was chosen for this study as it is quick, efficient and relies on basic assumptions of lichenometry while attempting to eliminate some biases related to anomalous lichen. It was also shown to be a reliable and accurate method (Bradwell 2009). In principle, the mean of diameters of the five biggest thalli of *R. geographicum* found on boulders building a moraine ridge is used to infer its age. Any thallus $\geq$20% bigger than the next in a dataset is removed as an outlier.

The selected boulders had uniform lithology (paragneiss) and were located on the distal slope of a ridge to avoid the cooling effect of catabatic winds from Helagsglaciären which would locally decrease the growth rate (Valladares and Sancho 1995; Winchester and Harrison 2000). That was also done to ensure that boulders that once crowned the crest but toppled over with time are also sampled as they were likely to host the oldest lichen; and to limit the probability of past lichen snowkill which would episodically offset the local growth curve back to zero (Benedict 1990, 1991; Lacelle et al. 2007). A few permanent snow patches are located near the proximal slopes of some moraines in the Helags cirque. Thus, restricting the sampling to the distal slopes would allow for controlling both the catabatic wind and lichen snowkill effects.

In order to construct the calibration curve, the nearest cemetery in Ljungdalen (62°51'17.3"N 12° 46'27.3"E; 18 km south-east from Helags valley) was investigated for old graves erected using local stone (paragneiss or granite), and 11 tombstones were sampled, the oldest having been erected in 1949. The website Svenska glaciärer – an inventory of Swedish glaciers (Bolin Centre for Climate Research 2017) – was also used, from which photographs of Helagsglaciären taken in 1895, 1908, 1930 and a scanned map published in 1969 were downloaded (see Kurop 2023 for the photographs; Enqvist 1910; Fries 1931; Lundqvist 1969). From these, moraine ridges at which the ice margin was located in the respective years were identified and sampled for lichen diameters. This resulted in a small dataset of independent age control on those particular moraines, with the oldest calibration point of 1895. A similar approach of using independent age control has been used in the European Alps (e.g. Carturan et al. 2014).

In order to extend the timeline even further, other lichenometric calibration curves were reviewed from research sites across Norway and Sweden. The best fit was found with the Eastern Jotunheimen (JotE) curve from Matthews (2005). This dataset extends about 250 years back in time and is based on historical measurements, photographs, maps and assumed ages of certain landforms due to several other lines of evidence pointing to it. The formula of the curve was modified by subtracting 20 from it to better fit calibration data in this study. The final form of the equation is

$$\log(y + 130) = 2.1916594 + 0.00353252x$$

where y is surface age and x is lichen diameter in mm. When tested on the calibration set, this equation resulted in calculated ages only 1–3 years different from the independently-calibrated ages within the Helags valley. This modified equation was then used to calculate the ages of all the sampled moraine ridges in the Helags valley that were outside the calibration dataset obtained locally.

3.4. Glacier and Equilibrium Line Altitude reconstruction

The ice margins had been established at six different time steps based on the lichen-derived chronology (c. 1960, 1930, 1890, 1790, ~700 and ~100 CE). The outline of the palaeoglacier was reconstructed in three dimensions using an established method discussed below.

There are two approaches that have commonly been used for that purpose. The first includes using an empirical equation to automatically extrapolate the glacier long profile from an outermost moraine (e.g. Pellitero et al. 2016); this method has benefits in topographic settings that are fairly simple, such as cirque or valley settings and where other ice-marginal constraints such as trimlines, meltwater channels etc. are lacking. Equally, the method is very powerful in studies where larger datasets of individual reconstructions need to be compared from a palaeoclimatic perspective (e.g. Rea et al. 2020). In complex mountainous settings such as ice-cap landsystems (e.g. Boston and Carr 2015; Chandler et al. 2019) and smaller cirque glacier settings where the geomorphological evidence enables a very detailed reconstruction of individual recessional stages (Chandler and Lukas 2017), the automated method is much less reliable than what has been termed the 'cartographic approach' (Pellitero et al. 2015, p. 61). In addition, because Helagsglaciären is still extant

and can be used to reconstruct its previous extent in a step-by-step fashion moving backward in time (cf. Lukas 2007), we have opted to use the latter approach for these reasons.

The approximate glacier surface elevation contours were drawn manually in QGIS 3.28 at 10 m intervals for each time step and then converted to a Digital Elevation Model (DEM) with 1 m resolution. The DEMs were then used to calculate the Equilibrium Line Altitude (ELA) at each time step using the Area-Altitude Balance Ratio (AABR) method by Osmaston (2005). As argued more extensively elsewhere, the AABR method was chosen over several other, cruder methods based on its superiority of including crucial factors like glacier hypsometry (e.g. Furbish and Andrews 1984; Benn and Gemmell 1997; Rea 2009; Benn and Hulton 2010).

The balance ratio (BR) reflects the ratio of slopes of net mass balance-altitude curves above and below the ELA. Rea (2009) calculated the 'typical' BRs for different kinds of glaciers across the world using the World Glacier Monitoring Service (WGMS) mass balance data. Out of this dataset, two AABRs are suitable for Helagsglaciären and thus are used in this study to calculate ELAs: the mid-latitude maritime AABR of 1.9 ± 0.81 and Western Norway AABR of 1.5 ± 0.4 (Rea 2009). The mean global AABR of 1.75 ± 0.71 by Rea (2009) was found to be statistically invalid in favour of the global median of 1.56 (Oien et al. 2022), and the latter is used here as a basis for the palaeo-precipitation reconstruction.

The transfer function to infer palaeotemperature and precipitation at an ELA was taken from Ohmura et al. (1992) who derived it from mass balance data of 70 globally distributed glaciers. As such, it is not ideal as the relationship between the summer temperature and annual precipitation depends on continentality of climate (Carr et al. 2010). However, there are no such relationships derived locally and thus the global dataset is the best available option to avoid circular reasoning (Benn and Ballantyne 2005; Lukas and Bradwell 2010; Boston and Carr 2015; Chandler and Lukas 2017). The equation

$$P_a = 645 + 296T_3 + 9T_3$$

represents the annual precipitation (P_a) at the ELA as a function of mean summer temperature (T_3 – June, July, August). This method has an uncertainty of ±200 mm (Ohmura et al. 1992).

The local mean summer temperature was taken from Zhang et al. (2016) who reconstructed it using tree rings at 650 m a.s.l. Their record spans the last 1160 years. An earlier Holocene July temperature value was taken from Velle et al. (2005) who derived it from chironomids from six lakes in Scandinavia, one of them being Lake Spåime 20 km north of Helags valley. The temperature and precipitation were adjusted to the ELA for the calculation, and sea level for later comparison using the mean lapse rates of 0.6°C/100 m and 8%/100 m (after Haakensen 1989).

4. Results and interpretation

4.1. Geomorphological mapping

The geomorphological map is presented in Figure 2. Helagsglaciären occupies an asymmetrical, ~2 km long valley with a 1.5 km wide cirque accommodating two almost-separate ice masses: a southern ice unit lying in a possibly overdeepened niche and a northern ice unit resting on a long, narrow (~300 m) bedrock bench. The southern ice unit extends into the glacially moulded and occasionally streamlined bedrock basin which descends in elevation from south to north. Some striae were noted with bearing parallel to the streamlining. The edge of the bedrock basin is topped by an extensive system of multi-crested, partly lobate moraine ridges built with subangular and angular boulders, out of which two main sets can be distinguished (R11 and R12-14). The southernmost fragment of this system (R6) is flattened, diffuse and appears to have flutes with an azimuth of about 045° on its surface in contrast to two crescent ridges below it (R10 and R10a). The southern part of the basin is flanked by a prominent lateral moraine (R9), the crest of which is descending down-valley and also seems to consist of two parts. A field of large angular boulders

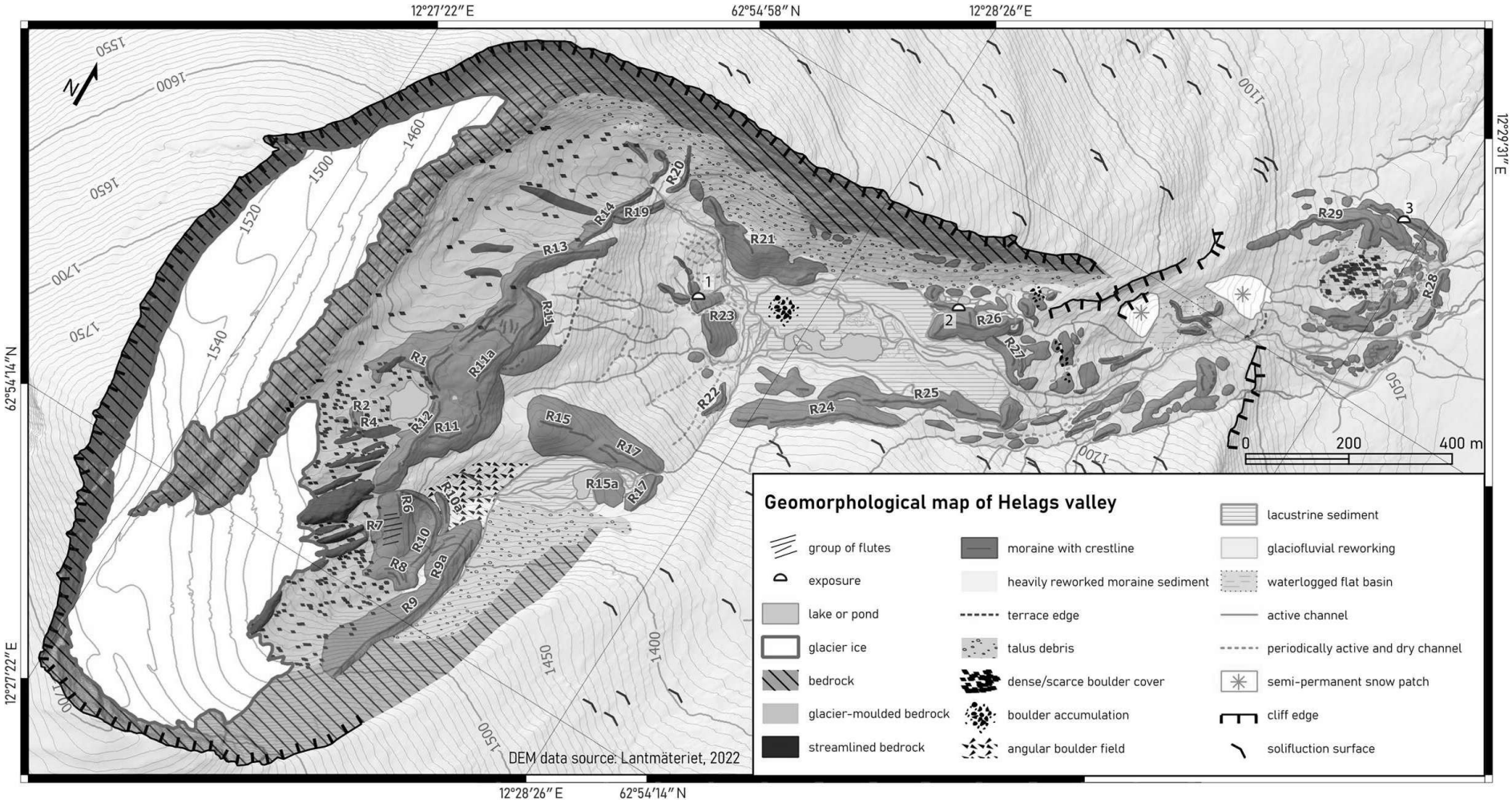

Figure 2. Geomorphological map of the Helags valley. The valley can be divided into two parts: the cirque or upper part where the current glacier is located and the lower part with a large lake plain bordered by two lateral moraines (R24-25) from the southern side. A set of two arcuate moraine ridges (R28-29) mark the maximum extent of Helagsglaciären's sediments in the Handölan valley. The names R1-R28 refer to moraine ridges sampled for lichenometry.

separates the moraines R9-R10a from a basin infilled with lacustrine and fluvial sediment. The basin ('upper lake plain' hereafter) is bordered by a large, broad and weathered lobate-shaped moraine (R15-17) that separates it from a long steep step (with an average slope of 35°) that dissects the Helags valley into two parts. Extensive talus debris is accumulated on the southern wall of the cirque.

The step between the upper and lower parts of Helags valley descends about 140 m and comprises heavily dissected and reworked diamictic sediment with occasional individual hummocks. Numerous active and periodic meltwater channels cut through this undulating surface. The step terminates on a large discontinuous asymmetric moraine ridge in which the first sediment exposure was dug (R23, exposure 1). The ridge has a long distal but very short proximal slope adjacent to a waterlogged flat basin.

The floor of the lower part of Helags valley, below the threshold described above, is at 1230 m a.s.l. and is mostly occupied by extensive lacustrine sediments ('lower lake plain' hereafter) partially reworked by streams and interrupted by a distinct boulder accumulation zone, a lake nested within them and two sets of lateral moraines running alongside it, parallel to the valley walls. The crestline of the outer lateral moraines (R24) follow the 1260 m contour while the inner ones' (R25) runs subparallel around 1250 m a.s.l. The southern set is much better preserved than the northern one, which was either eroded or covered by talus. Solifluction lobes are well developed on the sides of Helagsfjället outside the range of the lateral moraines. A couple of channels run along the distal slopes of the southern set of the moraines, occasionally cutting through them. The outer lateral moraine (R24) becomes progressively more fragmented down-valley. The lower lake plain is enclosed on its downvalley side by a low quasi-arcuate ridge with a gentle proximal slope and steep distal one (R27). The ridge is cut by the stream draining the lower lake plain and much of it is thus eroded. Directly to the north-east of the plain there is an area of unordered low-amplitude hummocks and periodically water-filled depressions, some linked with blindly-ending streams. It is restrained by a larger, branching elongated ridge (R26) that separates it from the lower lake plain. Exposure 2 was dug on R26's northern side. The area extends into a rocky shelf and is partly covered by talus.

The area extending downvalley from the lower lake plain is characterized by its steeper slope and common reworking and fragmentation of moraines by multiple streams. In the lower northern part of this sector there are two semi-permanent snow patches. The upper one sits in a deep niche underneath a rock cliff with waterlogged flat terrain in front of it while the lower one rests on a debris-covered slope of Helagsfjället.

Following another steep step, the sediments expand about 400 m beyond the Helags valley onto the floor of Handölan valley. The sediments form two sets of clear arcuate moraine ridges. The outer-most moraine (R28) is about 10 m high and dissected into individual linear ridges and hummocks by streams draining the Helags valley. It has an undulating crestline and occasional little dry channels incised into its outer slopes perpendicularly to the crestline. Exposure 3 was dug on the northern proximal slope of R28. The inner arcuate ridge is higher (R29, up to 20 m) and located at a 0–30 m distance from the outer one, with channels running between them. The inner set is characterized by multiple crestlines, some of them bifurcating, dry/waterlogged depressions and occasional fragmentation into hummocks by streams draining the interior of the lobe. The interior of the ridge itself comprises a series of semi-circular water-logged basins with clear terrace edges on the upglacier side, from which streams emerge. The entire interior area is covered in scattered boulders that range from 0.5 to 2 m in their a-axes.

4.2. Sedimentology

Three exposures (Figure 3) were dug and logged in three moraine ridges in the lower part of the Helags valley and Handölan valley (see Figure 2). The sediments in the upper part of the valley contained too many boulders to enable any logging.

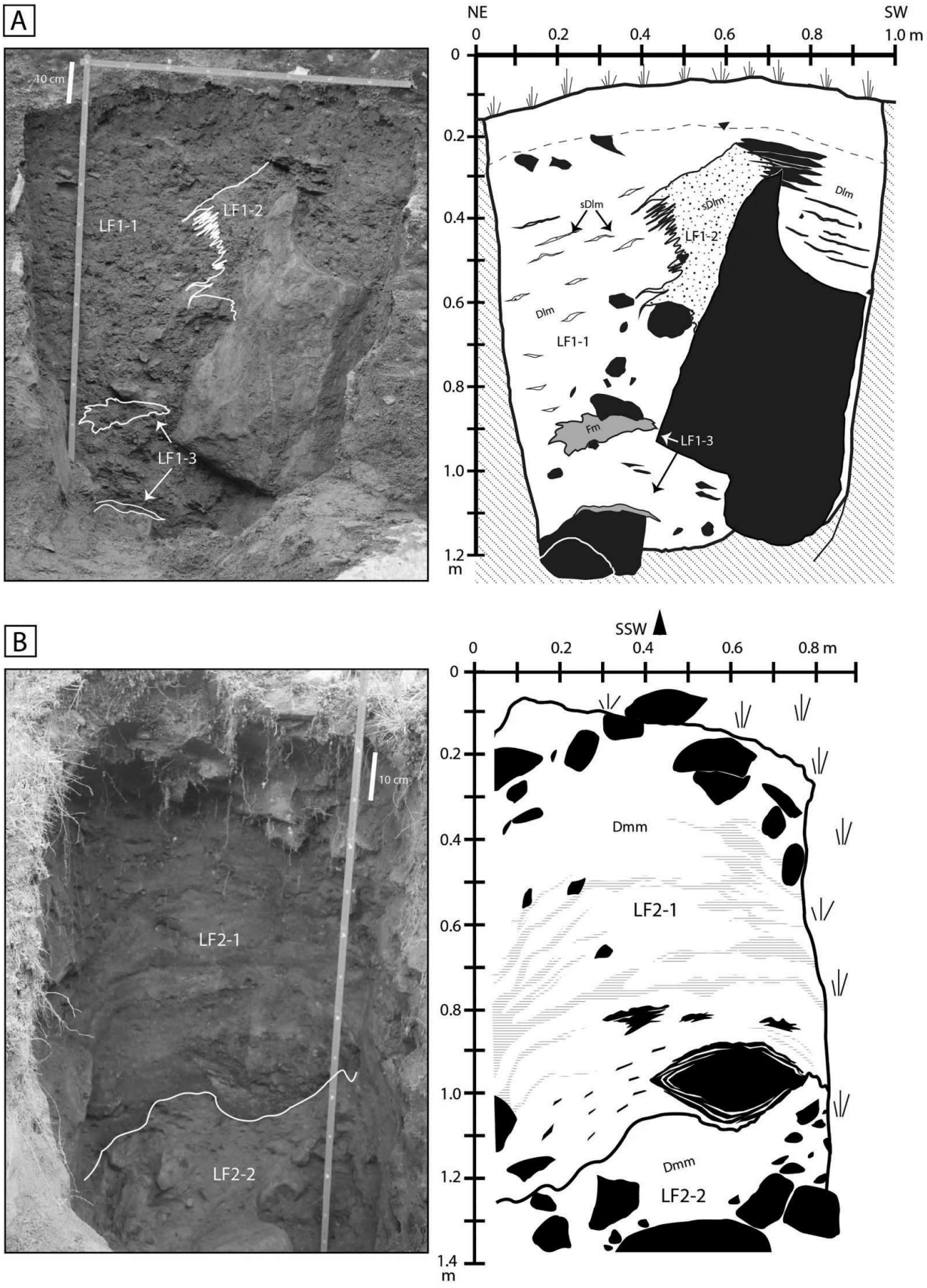

Figure 3. A – sedimentological log of exposure 1 dug in R23 (Figure 2 for location). LF refers to different lithofacies, as in the main text. B – sedimentological log of exposure 2 dug in R26. C. Sedimentological log of exposure 3 dug in R28. Frontal view (section I) and two wings (sections II and III) of a trench dug into the proximal side of the moraine ridge. Boulders are lettered for clarity of description and identification, e.g. boulder A in section I and II is the same boulder viewed from different angles; boulders E, F and G exhibit bullet-shaped morphology (as in main text).

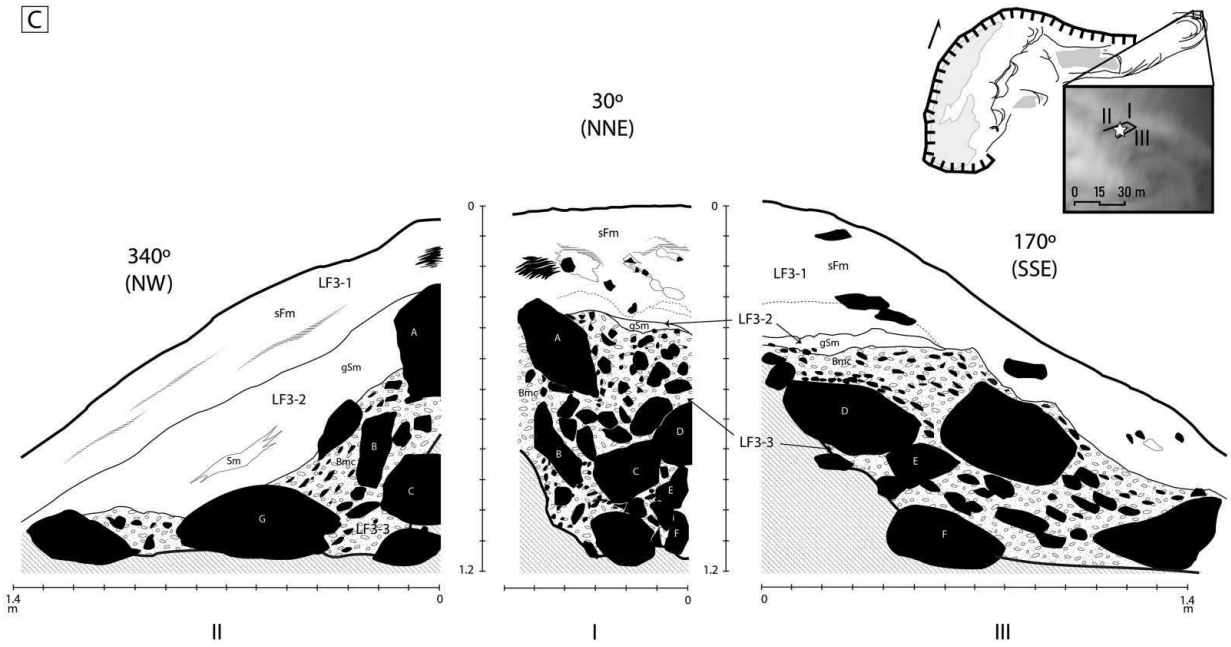

Figure 3. (Continued).

4.2.1. Exposure 1

This exposure (Figure 3a) was dug by excavating a wall of a channel incision in moraine R23. It is small (1 × 1.2 m) and shows an irregular arrangement of boulders in a finely laminated, weakly consolidated and matrix-supported diamict (LF1-1). The sense of lamination is given by long narrow streaks of sandy sediment in the upper, northern part of the exposure gently dipping NE, which gradually become more poorly-sorted sandy pockets with increasing depth. Nearly half of the exposure is occupied by a large sub-angular boulder with a protruding 'horn' on which a weathered clast is lodged. The sandy streaks dip gently towards SW on its southern side. On the northern side of the boulder the diamict becomes much more sandy (LF1-2) and extends outwards, interfingering with the less sandy matrix LF1-1. A few clasts are draped in this zone. A notable feature is a warped, elongated massive clay inclusion (LF1-3) on which a cobble is resting. A lens of similar clayey sediment is resting on a surface of another large boulder in the lower part of the section.

4.2.2. Exposure 2

This exposure (Figure 3b) was dug in the north-facing slope of moraine R26 and also has a small size (1 × 1.4 m). There are two distinctive lithofacies separated by a sharp undulating contact. The upper one (LF2-1) is a poorly sorted and weakly consolidated diamict of a rusty colour. There is a concentration of subangular boulders in the upper part of it which are absent from the middle and only reappear again near the contact, often as heavily weathered and easily crumbling clasts. Numerous blackish flame-like wisps are interspersed throughout this lithofacies. LF2-1 attains a more intense rusty colour in the ~5 cm directly above the contact.

The lower lithofacies (LF2-2) is a massive matrix-supported sandy clayey diamict that is much better consolidated than the upper one. It has a light brownish-grey colour and hosts subangular to subrounded interlocking boulders that increase in numbers downwards so that it was impossible to dig further than 1.4 m.

4.2.3. Exposure 3

This exposure (Figure 3c) consists of three sections roughly at right angles to each other and was dug in the proximal side of the northern fragment of ridge R28. The transect was dug 1.4 m into the moraine until the crest was reached, and so Figure 3c presents the frontal view (segment I) and two wings (segments II and III) of the resulting blind trench. The moraine consists of three lithofacies

resting on each other. LF3-1 is up to 30 cm thick and made of darkening up, rust-coloured sandy clayey silt. LF3-2 is a weakly consolidated gravelly silty sand that in segment III shows a faint lamination dipping downslope. There is a more sandy pocket within it interfingering with LF3-2 in segment II. A sharp undulating contact separates LF3-2 and LF3-3. LF3-3 consists of interlocking subangular and subrounded boulders with a sandy, angular gravel matrix between them. The entire sediment is very weakly consolidated and readily disintegrates at the slightest touch. The arrangement of boulders seems chaotic when viewed in segment I, though the long axes of many of them point downwards. When viewed in a profile (segments II and III), the boulders' long axes are arranged sub-parallel to the slope and give an impression of downslope alignment. Such weak stratification is also visible in the gravels of the matrix between the boulders that in some places even form distinct pavements resting on the top surface of a boulder (e.g. boulder D). Some boulders look bullet-shaped (e.g. F, E and G).

4.3. Integrated interpretation of the processes involved in the dynamics of Helagsglaciären

4.3.1. The Handölan valley

The outermost moraine (R28) is interpreted as having been built by loose debris flows (LF3-3) dumped from the ice margin during stable conditions, consisting of supraglacial (the angular gravel fraction) and subglacial (rounded boulders and bullet-shaped clasts) material. This interpretation is based on the mixed, unsorted clasts giving a chaotic impression but revealing a semi-arranged pattern indicative of flow downslope. A notable absence of deformation structures indicate that the material was deposited through passive release (dumping) and not disturbed by the ice margin anymore (by e.g. pushing), similarly to the process described by Krüger et al. (2002). The roundness of boulders and especially their bullet shapes indicate that active transport processes were present probably throughout the length of the glacier, which suggests warm-based conditions at most of the glacier's sole (Kleman et al. 1997). LF3-2 represents better-sorted and finer-grained sediment deposited on the moraine irregularly along the ice margin (varying thickness) by glaciofluvial processes. Occasional sand lenses might be evidence of lower-velocity channels on the surface of this dump moraine (cf. Krüger 1997; Lukas 2005). The silty, rusty soil layer capping the moraine (LF3-1) indicates that a long time has passed since the deposition of R28. The uneven, undulating crestline of R28 might point to the existence of former ice cores, suggesting a frozen ice margin at the time of deposition. The southern fragment of R28 displays a number of little dry channels incised into its slopes perpendicular to the crestline which might be a trace of meltwater runoff routes.

Several insights can be also gained from the pattern of crestline bifurcation of moraine ridges. In the Handölan valley, the planform of R29 is simply a smaller version of outermost R28, indicating an approximately uniform decrease in volume of the glacier's tongue (both along its front and sides). However, R29 moraine exhibits three crestline bifurcations which suggest a later more active retreat and a snout sensitive to changes in mass balance (Boston and Lukas 2019). That would further suggest deposition by a temperate glacier that was closely coupled to climate during this phase of overall retreat.

4.3.2. Lower part of the Helags valley

4.3.2.1. Evidence of cold-based ice. The two sets of prominent lateral moraines (R24-25) reach up to 40 m in height and are bordered by impressive meltwater channels cut into their distal sides in the adjacent non-glacial sediments. According to Benn and Evans (2010, p. 604), such distinct incisions are characteristic of a glacier margin frozen to the ground so that the meltwater cannot penetrate below it. It is typical for many cold-based glaciers where permafrost is common (Kleman et al. 1997; Greenwood et al. 2007), though it has also been documented at temperate glaciers (Syverson and Mickelson 2009).

Reinardy et al. (2019) have shown that temperate glaciers can contain areas of frozen bed where ice thickness is less than 10 m or where permanent snow rests on the surface of a glacier. These circumstances would result in englacial sediment transfer (thrusting or freeze-up) at the snout or development of hummocky controlled moraine. A similar process is suspected to have happened in the area north-east of the lower lake plain where exposure 2 was dug. The undulating contact between LF2-1 and LF2-2, diamictic chaotic sediment with many boulders of LF2-2 and hummocky (in descriptive terms) geomorphology with multiple small circular basins and blind channels suggest that this is a dead-ice meltout area. Similar structures have been reported from known dead-ice landforms (e.g. Evans and Benn 2021: Fig. G.27). Comparable topography inside the range of R28-29 moraines implies that some dead ice blocks might have detached there as well (cf. Kjær and Krüger 2001; Lukas 2011).

4.3.2.2. Evidence of active retreat. The western end of the lower lake plain contains a set of landforms suggestive of a single-front oscillatory ice margin of a temperate glacier. Most notably, the bifurcating crestline of R23 and the neighbouring fragments of lateral moraines (R21 and R25) implies a snout sensitive of mass balance changes (cf. to section 4.3.1) and, together with a set of meltwater channels running parallel to them, indicate an actively retreating glacier, similar to the evidence discussed by Boston and Lukas (2019). This is further supported by the laminated nature of LF1-1 in exposure 1, the draping of clasts and a warped stoss-lee clay rip-up clast which suggests that some degree of sediment deformation during overriding of previously deposited material was involved in building R23. This is consistent with an oscillating ice margin where liquid water is present to facilitate fast movement and dynamic advances and retreats. Additionally, fine-grained matrix building all the moraines in the lower part of the Helags valley indicate substantial subglacial grinding and transport possible only under a warm-based glacier.

4.3.2.3. Proglacial lakes. The glacier terminated in a proglacial lake (now the lower lake plain) created by abundant meltwater dammed by R27. The proglacial lake was probably too shallow for the glacier to reach its floatation point and thus to support a calving margin, but it cannot be ruled out that individual dropstones might be scattered throughout the plain. The presence of water at the ice margin almost certainly increased the dynamic retreat rates of the glacier locally (Carrivick and Tweed 2013; Sutherland et al. 2020). The boulder accumulation zone is therefore interpreted as boulders dumped off the ice margin during one of the retreat stages, in line with observations from modern ice margins that are temporarily stationary during overall retreat (Wyshnytzky et al. 2021; Rettig et al. 2023).

Subsequently, Helagsglaciären seems to have been divided into two individual flow units funnelling towards the lower part of the valley. The southern flow unit of the glacier produced another shallow proglacial lake (upper lake plain) dammed by R17. A branching arm of moraine R15 (R15a) running through the upper lake plain represents an oscillatory retreat stage similar to the boulder zone identified in the lower lake plain. Both proglacial lakes strongly suggest a temperate ice margin of an actively retreating glacier.

4.3.3. Upper part of the Helags valley

The upper part of the valley exhibits plenty of erosional forms (such as streamlined bedrock or striae) typical for debris-rich basal ice that is also warm-based because regelation (melting and freezing) must have happened to incorporate boulders into it (Benn and Evans 2010, p. 340). The streamlined bedrock indicates ice flow direction out of the valley. The different bearing of these forms in the northern and southern part of the cirque indicates that there were two independent lobes of Helagsglaciären. Striae noted on the surface of the bedrock point to basal sliding that would only be possible if liquid water was present (Lipovsky et al. 2019), suggesting that temperatures at the sole of the glacier reached the pressure-melting point (PMP).

The sinuous moraine ridges at the rim of the cirque (R12-13) reflect a multi-lobate gradually retreating ice front with several stillstands when conditions turned colder. Lack of meltwater channels between the crests and generally shared, undisturbed base of the moraines indicate that these are not active retreat features. The cirque's width is probably responsible for the very close spacing between individual crestlines as the glacier's response to mass balance changes was distributed across a wider ice front compared to the more enclosed lower part of the Helags valley. The angular and subangular boulders building these moraines suggest a predominant supraglacial debris transport route and deposition via dumping.

Several crestline bifurcations are found along the rim moraine R6-R20, implying three lobes or glaciologically distinct flow units (southern, middle and northern ice unit marked by R10, R11 and R19-20 respectively). Because of presence of striae on bedrock in the cirque, all of them seem to have been warm-based despite a significant size reduction of Helagsglaciären compared to its maximum limit. The three individual ice units probably only start acting as one when they coalesce as the ice gets funnelled towards the narrower part of the valley during times of sustained positive mass balance.

Observations of subrounded pebbles frozen to the sole of the southern part of the glacier suggest that subglacial erosion of the substrate is ongoing despite significant glacier reduction in recent years. Apart from that, the current ice margin contains a mixture of material from large subangular boulders embedded in ice or resting on top of it, to finer angular debris melting out from the ice surface in distinct bands. As such, the currently deposited sediments probably reflect input from all three transport routes – supraglacial, englacial and subglacial.

4.4. Lichenometry

The complete calibration curve, constructed based on the method reviewed above, is presented in Figure 4. It is based on eight calibration points and covers 127 years. The data fit the curve well (R^2

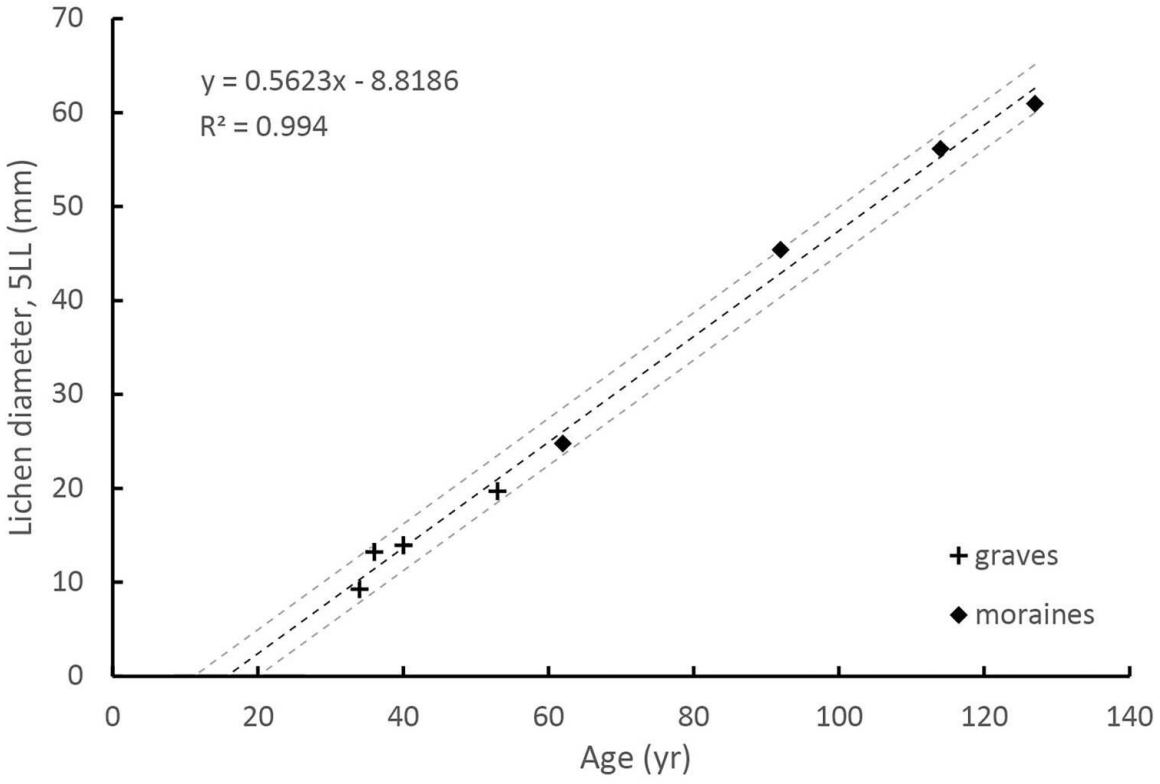

Figure 4. Lichen diameter-age calibration curve for Helagsglaciären's foreland. 5LL stands for the mean of the five largest lichens. Out of eleven sampled graves, only four were used as the others seemed apparently disturbed (e.g. cleaned) after preliminary plotting. The grey dashed lines mark the 95% confidence limit.

Table 1. Calculated ages of landforms in the Helags valley. JotE refers to ages calculated using the modified Eastern Jotunheimen curve of Matthews (2005). Historical year is based on the moraine identification from historical photographs. Error values (±) reflect 1 std as evaluated in Matthews (2005). Surfaces substantially older than the oldest calibration point have an unknown error (?).

ID	Lichen diameter (5LL, mm)	Age (yr) JotE	Year CE (JotE)	±	Hist. year
R4	19.66	52	1970	5.7	
R5	24.74	60	1962	5.7	1960
R6	45.4	95	1927	5.7	1930
R6	44.1	93	1929	5.7	1930
R7	8.36	36	1986	5.7	
R8	41.94	89	1933	5.7	
R8 (gully)	59.04	121	1901	5.7	
R9	71.72	149	1873	5.7	
R9a	103.04	229	1793	34.5	
R10	60.94	125	1897	5.7	1895
R11	104.26	233	1789	34.5	
R11a	85.44	182	1840	34.5	
R12	56.12	115	1907	5.7	1908
R13	85.74	182	1840	34.5	
R14	72.56	151	1871	34.5	
R15	224.4	835	1187	?	
R17	268.2	1247	775	?	
R20	84.32	179	1843	34.5	
R21	253.4	1091	931	?	
R23	201.8	673	1349	?	
R24	330.2	2151	129 BCE	?	
R25	333.0	2203	181 BCE	?	
R26	221.0	808	1214	?	
R28	315.8	1899	123	?	

= 0.994), which gives confidence in lichenometry being reliable in the Helags valley. This curve was then used to extend the chronology according to equation 1 (see section 3.3).

The calculated ages and corresponding years for different landforms in the Helags valley are presented in Table 1. They range from 52 years for moraines closest to Helagsglaciären to over 2000 years for the southern lateral moraines. The general trend yields increasing ages with distance from the glacier. However, a few exceptions to this appear in the lower level of the Helags valley and the Handölan valley (e.g. R23, R25, R26). The ages agree very well with the moraines used for calibration (R5, R6, R10 and R12), instilling confidence in the results from the upper part of the Helags valley. The most distant and oldest moraine ridges from that part (R11 and 9a) yield ages of 233 and 229 years, which correspond to years 1789–1793 CE, about 100 years older than the oldest calibration point. Other consistent age groups imply moraine deposition around 1840 CE (R20, 13 and 11a), 1870 CE (R14 and 9), 1900 CE (R12, 10 and R8) and 1930 CE (R8 and 6).

The credibility of the data decreases significantly for the sediments in the lower part of the Helags valley due to the lack of calibration points, increased fragmentation and reworking of landforms, and increased difficulty in finding suitable lichen that have not demonstrably coalesced. This is manifested in age reversals (e.g. the inner lateral moraine R25 yields an older age than the outer one R24; R26 is younger than sediments upvalley) and age inconsistency of data points from the same landform (e.g. the outermost R28 and outer lateral moraine R24 both mark the same limit but R28 is younger than R24 if taken at face value). The lichen in the lower part of the valley were commonly irregularly shaped or were found to have coalesced with others. While such individuals were avoided, there is a risk that the suture zone between two lichen was unrecognizable and thus a pair (or group) of lichen was sampled as one. This would give highly erroneous ages, a risk that increases with age (Bradwell 2010).

Another point of caution is the reworking of sediments that would topple over and bury boulders from the crest of a ridge and expose new boulder surfaces for lichen colonization. This is a common

Table 2. Calculated ELAs from Helags valley, using the AABR method of Osmaston (2005) and accumulation-ablation balance ratios of three different glacier types after Rea (2009)[1] and Oien et al. 2022.[2] The columns on the right side of the table present temperature from Zhang et al. (2016) and Velle et al. (2005)* adjusted to the ELA using 0.6°C/100 m temperature lapse rate (T at ELA); and calculated precipitation at the ELA (AABR of 1.56; P at ELA). Both are adjusted to the sea level for comparison (last two columns) using the temperature lapse rate mentioned above and precipitation lapse rate of 8%/100 m (after Haakensen 1989).

	ELA (m a.s.l.)									
Period	1.9[1]	±	1.5[1]	±	1.56[2]	±	T at ELA (°C)	*P* at ELA (mm)	T at sea level (°C)	*P* at sea level (mm)
Early Holocene*	1369	39	1386	21	1383	36	3.81	1905	12.11	904
c. 700–1200	1465	20	1474	11	1472	19	3.06	1634	11.89	750
1790s	1490	16	1497	9	1496	16	2.75	1526	11.72	695
1900s	1498	16	1505	11	1504	14	2.91	1582	11.93	718
1930s	1486	16	1492	9	1491	15	3.79	1898	12.74	865
1960s	1499	14	1505	8	1504	13	3.80	1901	12.83	863

source of error on latero-frontal moraines (Humlum 1978; Lukas et al. 2012). This process is suspected on R23 and R21 as the former lies at the foot of a steep slope with multiple streams fragmenting it and thus the age of 673 years (deposited in 1349 CE) is at best an estimate of the boulder exposure age but not deposition. The latter lies under a steep cliff, is reworked and partly buried.

Due to the uncertainties tied to the measurements in the lower part of the valley, the resultant numerical ages from there are discarded and landforms R21-28 are from now on referred to as simply *early Holocene in age*.

A special case is made for R15-17 which refer to two parts of the same lobate structure delineating the upper lake plain. Due to their different morphology, they are likely to represent two different events which is supported by resultant years of deposition in around 1187 (R15) and 775 CE (R17) and spatial arrangement (the older one is further from the glacier snout). However, large uncertainty is placed on them because of the age limit of the method and lack of calibration points in the immediate vicinity.

Based on the age modelling, the ice margin could be drawn at six time periods: early Holocene (maximum advance), 700–1200 CE, 1790s CE, 1900s CE, 1930s CE and 1960s CE; these ages are used for the following ELA reconstructions.

4.5. Equilibrium line altitude and palaeoclimate reconstruction

The ELAs for respective time periods and glacier types are presented in Table 2. Within the error limit, they show a rising trend from about 1370 m a.s.l. during the early Holocene advance to about 1510–1500 m a.s.l. in the twentieth century. The ELA was only about 20 m lower during the local LIA maximum than at present. The values differ by up to 17 m between the AABRs (as in Rea [2009] and Oien et al. [2022]), but the difference is more typically less than 10 m. The lowest ELAs are for 1.9 AABR while the highest – for the 1.5 AABR. The 1930 and 1960 values were calculated due to the availability of glacier hypsometry data at those times. However, Helagsglaciären was then experiencing a rapid thinning and retreat and thus was not in equilibrium. Therefore, these values should be treated with great caution as long-term averages of the glacier's mass balance conditions in the twentieth century.

The columns on the right-hand side of Table 2 show the calculated temperature and precipitation values for the selected time periods. The temperature oscillated within a 1.1°C-difference. The lowest summer temperature was for 1790s CE (LIA maximum), however that period also seems to be the driest of all. The early Holocene advance was 0.4°C warmer but had a 200 mm higher precipitation at the sea level, which makes it the wettest period of all. The 700–1200 CE advance was nearly equally cold as the 1790s but 50 mm wetter. The last LIA advance – around 1900 CE – was almost as cold as in 700–1200 CE but slightly drier. The twentieth century experienced warmer and wetter conditions.

5. Discussion

5.1. Changing dynamics of a small valley glacier

Throughout the Holocene, Helagsglaciären experienced a lot of changes in its mass balance due to changing climate. As a result, its dynamics and geomorphological imprint on the landscape also changed. However, based on the geological evidence, the glacier's thermal regime appears to have remained remarkably consistent for most of the Holocene, likely because of its small size and location at the lower latitudes in the Scandinavian Mountains. During periods of larger extent, the evidence discussed in sections 4.3.1 and 4.3.2 suggests that Helagsglaciären was a polythermal glacier with an active and climatically-sensitive snout that was only frozen to the ground near the margins where ice was thin, similar to the glaciers currently found in high Arctic areas (Irvine-Fynn et al. 2011) or southern Norway (Reinardy et al. 2019). Once the ice retreated to position R23, the climate was warm enough and the funnelled ice was likely thick enough for PMP to be reached throughout, resulting in an actively oscillating ice margin (section 4.3.2). The glacier exhibited an entirely temperate regime up until the twentieth century when it got gradually fragmented into first three, then two independent flow units – a northern and southern one. The northern unit is currently stagnating and probably cold-based while the southern unit is active and warm-based (section 4.3.3) but may soon transition to being cold-based due to rapid thinning. A change in ice thickness has been identified as a major factor determining a change in thermal regime in many contemporary glaciers throughout the Arctic (Mooers 1990; Reinardy et al. 2013, 2019; Tonkin et al. 2016; Mallinson et al. 2019).

A considerable influence on the dynamics of Helagsglaciären is the glacier's hypsometry and valley topography. Funnelling of ice once it exits the cirque makes the ice margin particularly sensitive to changes in mass balance when it reaches the narrower lower part of the valley, resulting in widely spaced moraine ridges. In the upper part of the valley the response to climatic changes results in only a slight retreat/advance due to much wider ice front. Similar conclusions were reached by Kuhn et al. (1985) in the study of Alpine glaciers. The factor of topography should be carefully taken into account when interpreting a valley/cirque glacier's behaviour from its moraine sequences.

5.2. Chronology

The presented lichenometric chronology for sediments in the Helags valley is not complete because the moraines beyond the cirque pre-date the upper limit of the method. However, several important points can be deduced from it.

The Helags valley represents deposits from glaciations far earlier than the LIA, which is in agreement with Bergström (1955) and Lundqvist (1969) and disagreement with the widely-held consensus that glaciers in Scandinavia reached their Holocene maxima during the LIA (Karlén 1973; Nesje 2009). For Helagsglaciären, its LIA expansion was constrained only to the upper part of the valley and the glacier reached its maximum in about 1789 CE, with other notable readvances in around 1840, 1870 and 1890 CE. From that point, there was an overall retreat marked by extensive ridges deposited in the 1900s and 1930s. By the 1960s, Helagsglaciären had disintegrated into two units, with the southern one still actively eroding and dumping sediment on an exposed overdeepened bedrock niche at the time of the fieldwork. However, even this active lobe has not produced a well-marked moraine ridge, indicating that the entire system has been in negative mass balance throughout the recent decades, which is consistent with mass balance data for Helagsglaciären for 1999–2019 from the World Glacier Monitoring Service (WGMS 2021).

The upper proglacial lake plain is framed by a two-phased latero-frontal moraine R15/17. The ages span 1.3–0.8 ka BP which would be at the upper limit of the dating method and therefore should be regarded with caution. However, glaciers are known to have expanded in Scandinavia

around that time (Rosqvist et al. 2004) and thus the ages of these landforms are regarded as at least broadly accurate. Similar results were observed at Austre Okstindbreen 300 km north of Helagsglaciären, where an advance around 1.3 ka BP was found to correspond to the Neoglacial maximum, while the LIA extent was smaller (Bakke et al. 2010).

The earlier Holocene sediments in the lower part of the Helags valley and in the Handölan valley remain unconstrained. Given these circumstances, in the following section this study attempts to narrow down the possible timing of the outermost deposits by means of comparison with other climatic and geomorphological records from Scandinavia.

5.3. Palaeoclimate reconstruction

Numerous sources from Scandinavia point to a severe climatic cooling and very wet conditions centred around the Finse event around 8.2 ka BP (Nesje et al. 2000; Snowball et al. 2002, 2010; Hammarlund et al. 2004; Bergman et al. 2005; Seppä et al. 2005; Velle et al. 2005; Antonsson and Seppä 2007; Sundqvist et al. 2007; Nesje 2009). Helagsglaciären advanced 2.6 km from the cirque's headwall during the early Holocene, compared to current glacier length of 0.4 km. This sixfold increase in length, combined with the cold and wet palaeoclimate reconstructed from ELAs in this study and considerable weathering of moraines R28-29 are consistent with deposition during the 8.5-8 ka BP cooling well-documented in this region (central-west Sweden) e.g. in lake sediments (Snowball et al. 2002, 2010; Bergman et al. 2005), cave deposits (Sundqvist et al. 2007) and tree-line lowering (Öberg and Kullman 2011). The tree megafossils from Helags valley collected by Öberg and Kullman (2011) and Kullman and Öberg (2020) were all dated directly outside of the 8.5–8.0 ka BP age range, suggesting climatic cooling at the site around the time of the Finse event (8.2 ka BP). Therefore, this age is proposed here for lateral moraines R24-25 and the outermost moraines R28-29.

Climate varied considerably during the 700–1200 CE (1.3–0.8 ka BP). Pronounced cooling was inferred around 1.2–1.0 ka BP (Rosqvist et al. 2004; Zhang et al. 2016). This was followed by the Medieval Warm Period (Linderholm 2005; Zhang et al. 2016) during which the glaciers probably retreated. The climate was wet as inferred by Gunnarson et al. (2003) and reconstructed by Olsen et al. (2012) and Bakke et al. (2008), which all agree well with the climatic parameters calculated from Helagsglaciären's ELA at the R15/17 limit. Therefore, the interpreted age of R15/17 is narrowed here to span 1.2–1.0 ka BP (ninth to tenth century CE).

It has been suggested that Scandinavia experienced a very variable climate during the LIA (Nesje et al. 2007; Rosqvist et al. 2013), with the coldest periods around the years 1600, 1750, 1770, 1840, 1870 and 1900 CE. Some of these periods have resulted in the production of distinct moraine sequences (e.g. Nesje et al. 2007; Bakke et al. 2010; Zhang et al. 2016). Zhang et al. (2016) is a local dendrochronological temperature reconstruction covering the last 1200 years, where the summer temperatures deviated by about -1°C from the 1960–1990 mean during the coldest periods mentioned above. This agrees very well with Helagsglaciären's advances around 1790, 1840, 1870 and 1900 inferred from dated moraines R8, R10, R11, R13, R14 and R20 (Table 1).

Reconstructing palaeoprecipitation during the LIA is more problematic because wetness of an environment, apart from atmospheric factors, is heavily dependent on its hydrological regime which might be difficult to characterize in detail. This results in the lack of agreement between authors using proxies with different sensitivities to palaeoprecipitation.

According to Gunnarson et al. (2003) who derived his wetness reconstruction from Stömyren peat bog in south-central Sweden and a dendrochronological dataset, the time around 1790 CE experienced very wet conditions, which is in disagreement with the results in this study implying the period was the driest of all. However, other authors found weaker westerlies (Bakke et al. 2008) and a more negative North Atlantic Oscillation (NAO) index during the LIA (Olsen et al. 2012), both implying less humid conditions in western Scandinavia at this time which conforms to the climatic results from Helagsglaciären. Bakke et al. (2008) used sediments from proglacial lakes fed by small glaciers with short response times along the coast of Norway and calculated

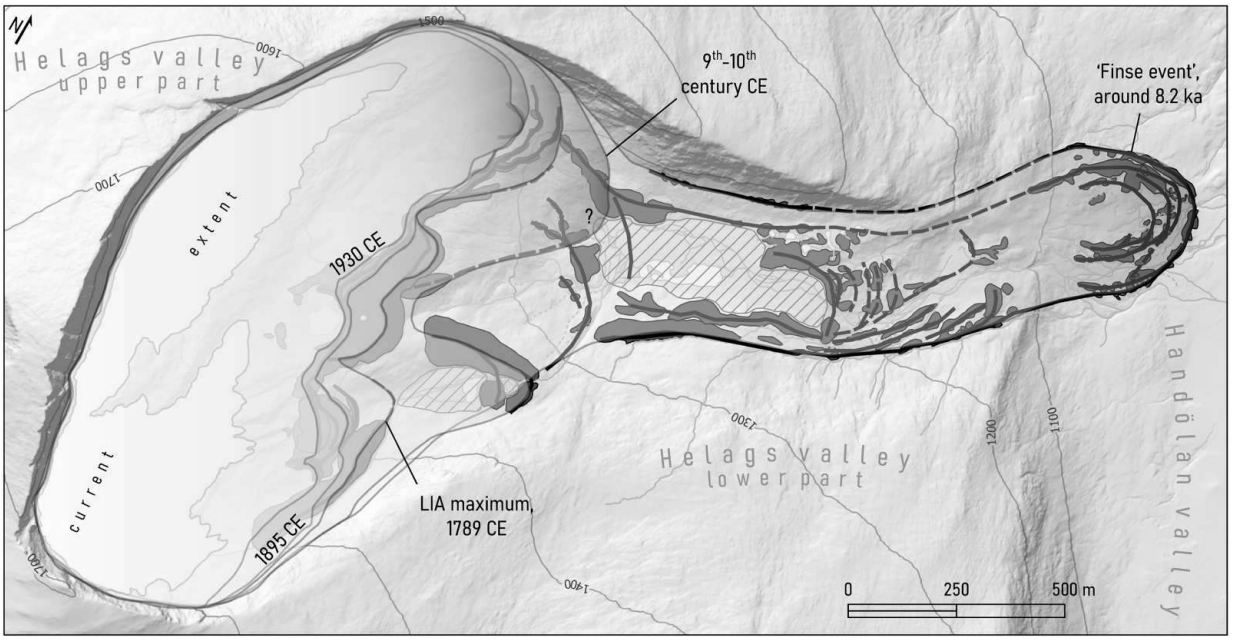

Figure 5. A synthesis figure showing the final interpretation of the chronology of retreat of Helagsglaciären. Grey polygons are mapped moraines from Figure 2. The thick black lines trace moraine crestlines. Dashed lines show where tracing of crestlines is uncertain. Hashed polygons represent the location of palaeo-proglacial lakes.

the ELAs of these glaciers. This proxy has a higher resolution than Gunnarson et al. (2003) and is more similar to the methodology employed here, so it is considered more relevant for comparison of precipitation totals. Olsen et al. (2012) used a lake sediment core from Greenland to reconstruct hypoxia and link it to lake water circulation changes indicative of changes in precipitation. Their reconstruction does not cover the year 1790 CE, however, it agrees very well with Bakke et al. (2008) and shows a decrease in NAO strength at the beginning of the LIA.

All reviewed studies agree that the period around 1.3–0.8 ka was wet or wetter than the LIA (Nesje et al. 2000; Gunnarson et al. 2003; Bakke et al. 2008; Andersson et al. 2010; Andersson and Schoning 2010; Olsen et al. 2012; Rosqvist et al. 2013). Nesje et al. (2000) present the only study that addresses precipitation during the Finse event (8.2 ka BP) and also reconstructs very wet conditions at that time, similarly to the results from Helagsglaciären.

It is concluded that precipitation reconstruction from Helagsglaciären matches other records well, which is significant considering the glacier's small size and strong influence of topography on its dynamics, and in particular the challenges provided by the limited datasets for comparison. Our dataset thus adds considerable value to our collective understanding of palaeoclimatic conditions in the southern Scandinavian Mountains and fills a gap that cannot easily be filled by other proxies.

5.4. Helagsglaciären and Holocene palaeoglacial reconstructions

Helagsglaciären is the first glacier in Sweden for which a complete Holocene reconstruction has been attempted using both geomorphological mapping and ELA reconstruction, the results of which are summarized in Figure 5. Previous works on the topic either focused only on the LIA (Regnéll 2016) or just the mapping (Karlén 1973; Karlén and Denton 1976). Several insights can be pointed out.

The dynamics of a medium-sized to small glacier can change through time due to combined effects of changes in climate and ice hypsometry, so that it is less or more responsive to the same climatic signal than those in the vicinity. A large influence on the timing of such a switch is possibly exerted by the overall size of the ice body (and especially thickness) which determines

absolute mass loss or gain, but also response time at the snout (Bahr et al. 1998). The southern location of Helagsglciären probably determined its switch from polythermal to temperate regime, unlike current polythermal Arctic glaciers that switch to cold-based thermal regime as they thin in a warming climate (Glasser and Hambrey 2001).

Helagsglaciären seems to be more sensitive to changes in precipitation than temperature. Both the 8.2 and 1.2–1.0 ka BP glacier advances were more extensive than the LIA limit due to wetter palaeoclimate, despite being warmer than the LIA. Therefore, Helagsglaciären is comparable to maritime Norwegian glaciers (e.g. Nesje et al. 2007; Jansen et al. 2016) regardless of its more continental location. That stresses the need for more accurate and complete reconstructions of winter precipitation for better understanding of past glacier oscillations.

There is a wide-spread recognition that the behaviour of small cirque or valley glaciers may be heavily dependent on non-climatic factors like topography or snowblow and thus not conform to, or reflect general palaeoclimatic changes (Barr and Lovell 2014). However, palaeoclimatic reconstruction at Helagsglaciären agrees well with other records from Scandinavia, though a larger investigation involving a group of nearby glaciers would be necessary for more robust assessment. This warrants more attention to be paid to other similar glaciers in future palaeoclimatic studies.

6. Conclusions

This is the first study in Sweden that attempted to fully reconstruct dynamics, chronology and palaeoclimate of a glacier throughout the Holocene by combining four complementary methods: geomorphological mapping, sedimentology, lichenometry and ELA calculation.

The Helags valley sediments were mapped in detail and 21 moraines were dated by lichenometry (R4-R15, R17, R20-26 and R28) using a locally-derived calibration curve. Based on the comparison of palaeoclimatic data from Helagsglaciären and other studies from Scandinavia, it is suggested that Helagsglaciären reached a Holocene maximum probably around the Finse event (8.5–8.0 ka BP) when summer temperatures were slightly warmer than during the LIA, but the climate was much wetter. Other prominent advances were around 1.2–1.0 ka BP, around 1790 CE (the LIA maximum) and 1900 CE, as inferred from lichenometry. The glacier switched from polythermal in the past to a temperate thermal regime today. It disintegrated into two parts, one of which is still active despite its small size.

The LIA was the coldest and driest period out of the established chronology. Helagsglaciären did not reach its Neoglacial maximum at that time, but earlier around 1.2–1.0 ka BP, similar to some glaciers in Norway which might suggest they were influenced by the same climatic stimuli.

Helagsglaciären responded to broader climatic trends, which encourages using small cirque and valley glaciers in similar palaeostudies. However, a regional approach including nearby cirque glaciers in Sylarna would be necessary to produce a more robust Holocene palaeoclimatic assessment for the southern Scandinavian Mountains.

Acknowledgements

AK would like to thank Oleg Zheleznyy for help with fieldwork.

Disclosure statement

No potential conflict of interest was reported by the author(s).

Funding

The lead author received Lund University's funding for master theses to organize fieldwork supporting the research in this article.

Notes on contributors

Anna Kurop is a PhD researcher at University of Stirling working on rapid deglaciation and sea level change on the Outer Hebrides, Scotland. Before, she completed BSc in Environmental Geoscience at the University of Edinburgh and MSc in Quaternary Geology at Lund University, both with projects focusing on reconstructing past glaciers.

Sven Lukas is Associate Professor in Glacial Geology at Freiburg University and aims to understand the formation, sediment properties and palaeoclimatic implications of sediment-landform through the study of active glacial processes in Arctic and Alpine regions. He gained his PhD from the University of St Andrews (Scotland) and his MSc from the Ruhr-University of Bochum (Germany).

Data availability statement

There is no other data used in this study than already stated in the manuscript.

References

Andersson S, Rosqvist G, Leng MJ, Wastegård S, Blaauw M. 2010. Late Holocene climate change in central Sweden inferred from Lacustrine stable isotope data. J Quat Sci. 25(8):1305–1316. doi:10.1002/jqs.1415.

Andersson S, Schoning K. 2010. Surface wetness and mire development during the late Holocene in central Sweden. Boreas. 39:749–760. doi:10.1111/j.1502-3885.2010.00157.x.

Antonsson K, Seppä H. 2007. Holocene temperatures in Bohuslän, Southwest Sweden: a quantitative reconstruction from fossil pollen data. Boreas. 36(4):400–410. doi:10.1080/03009480701317421.

Armstrong RA. 2016. Lichenometric dating (lichenometry) and the biology of the lichen genus Rhizocarpon: challenges and future directions. Geogr Ann Series A Phys Geogr. 98(3):183–206. doi:10.1111/geoa.12130.

Bahr DB, Pfeffer WT, Sassolas C, Meier MF. 1998. Response time of glaciers as a function of size and mass balance: 1. Theory. J Geophys Res Solid Earth. 103(B5):9777–9782. doi:10.1029/98jb00507.

Bakke J, Dahl SO, Paasche Ø, Riis Simonsen J, Kvisvik B, Bakke K, Nesje A. 2010. A complete record of Holocene Glacier variability at Austre Okstindbreen, Northern Norway: an integrated approach. Quat Sci Rev. 29(9–10):1246–1262. doi:10.1016/j.quascirev.2010.02.012.

Bakke J, Lie Ø, Dahl SO, Nesje A, Bjune AE. 2008. Strength and spatial patterns of the Holocene wintertime westerlies in the NE Atlantic region. Glob Planet Change. 60(1–2):28–41. doi:10.1016/j.gloplacha.2006.07.030.

Barnekow L. 2000. Holocene regional and local vegetation history and lake-level changes in the Torneträsk area, northern Sweden. J Paleolimnol. 23:399–420. doi:10.1023/A:1008171418429.

Barr ID, Lovell H. 2014. A review of topographic controls on moraine distribution. Geomorphology. 226:44–64. doi:10.1016/j.geomorph.2014.07.030.

Benedict JB. 1990. Lichen mortality due to late-lying snow: results of a transplant study. Arct Alp Res. 22(1):81–89. doi:10.1080/00040851.1990.12002767.

Benedict JB. 1991. Experiments on lichen growth II. Effects of a seasonal snow cover. Arct Alp Res. 23(2):189–199. doi:10.1080/00040851.1991.12002836.

Benedict JB. 2009. A review of lichenometric dating and its applications to archaeology. Am Antiq. 74(1):143–172. doi:10.1017/s0002731600047545.

Benn DI, Ballantyne CK. 2005. Palaeoclimatic reconstruction from Loch Lomond readvance glaciers in the West Drumochter Hills, Scotland. J Quat Sci. 20(6):577–592. doi:10.1002/jqs.925.

Benn DI, Evans DJA. 2010. Glaciers and glaciation. London: Routledge.

Benn DI, Gemmell AMD. 1997. Calculating equilibrium-line altitudes of former glaciers by the balance ratio method: a new computer spreadsheet. Glac Geol Geomorphol. 7. http://ggg.qub.ac.uk/ggg/papers/full/1997/tn011997/tn01.html

Benn DI, Hulton NRJ. 2010. An Excel (TM) spreadsheet program for reconstructing the surface profile of former mountain glaciers and ice caps. Comp Geosci. 36(5):605–610. doi:10.1016/j.cageo.2009.09.016.

Bergman J, Hammarlund D, Hannon G, Barnekow L, Wohlfarth B. 2005. Deglacial vegetation succession and Holocene Tree-limit dynamics in the Scandes Mountains, west-central Sweden: Stratigraphic Data compared to megafossil evidence. Rev Palaeobot Palynol. 134(3–4):129–151. doi:10.1016/j.revpalbo.2004.12.005.

Bergström E. 1955. Studies of the variations in size of Swedish glaciers in recent centuries. Union Géodés Géophys Int Assoc Int d'Hydrol. 39:356–366.

Beschel R. 1955. Individuum und Alter bei Fletchten [Individuality and age of lichens]. Phyton. 6:59–68.

Beschel R. 1957. Lichenometrie im Gletschervorfeld [Lichenometry in the glacier foreland]. Jahrbuch zum Schutze der Alpenpflanzen Tiere. 22:164–185.

Beschel R. 1958. Flechtenvereine der Stadte, Stadtflechten und ihr Wachstum [Lichen associations in cities, city lichens and their growth]. Ber Natwiss Med Ver Innsbr. 52:1–158.

Blomdin R, Becher GP, Smith CA, Regnéll C, Öhrling C, Goodfellow BW, Mikko H. 2021. Beskrivning till geomorfologiska kartan, Jämtlands län. Report K705. March: Sveriges Geologiska Undersökning.
Bolin Centre for Climate Research. 2017. Svenska glaciärer: Helagsglaciären. Accessed 9 May 2022. https://bolin.su.se/data/svenskaglaciarer/glacier.php?g=62.
Boston CM, Carr LS. 2015. A younger Dryas plateau icefield in the Monadhliath, Scotland, and implications for regional palaeoclimate. Quat Sci Rev. 108:139–162. doi:10.1016/j.quascirev.2014.11.020.
Boston CM, Lukas S. 2019. Topographic controls on Plateau Icefield recession: insights from the younger Dryas Monadhliath Icefield, Scotland. J Quat Sci. 34(6):433–451. doi:10.1002/jqs.3111.
Bradwell T. 2009. Lichenometric dating: a commentary, in the light of some recent statistical studies. Geogr Ann Series A Phys Geogr. 91(2):61–69. doi:10.1111/j.1468-0459.2009.00354.x.
Bradwell T. 2010. Studies on the growth of Rhizocarpon geographicum in NW Scotland, and some implications for lichenometry. Geogr Ann Series A Phys Geogr. 92(1):41–52. doi:10.1111/j.1468-0459.2010.00376.x.
Bradwell T, Armstrong RA. 2007. Growth rates of Rhizocarpon geographicum lichens: a review with new data from Iceland. J Quat Sci. 22(4):311–320. doi:10.1002/jqs.1058.
Carr SJ, Lukas S, Mills SC. 2010. Glacier reconstruction and mass-balance modelling as a geomorphic and palaeoclimatic tool. Earth Surf Process Landforms. 35(9):1103–1115. doi:10.1002/esp.2034.
Carrivick JL, Brewer TR. 2004. Improving local estimations and regional trends of Glacier Equilibrium Line altitudes. Geogr Ann Series A Phys Geogr. 86(1):67–79. doi:10.1111/j.0435-3676.2004.00214.x.
Carrivick JL, Tweed FS. 2013. Proglacial lakes: character, behaviour and geological importance. Quat Sci Rev. 78:34–52. doi:10.1016/j.quascirev.2013.07.028.
Carturan L, Baroni C, Carton A, Cazorzi F, Fontana GD, Delpero C, Salvatore MC, Seppi R, Zanoner T. 2014. Reconstructing fluctuations of La Mare Glacier (eastern Italian Alps) in the late Holocene: new evidence for a little ice age maximum around 1600 AD. Geogr Ann Series Phys Geogr. 96(3):287–306. doi:10.1111/geoa.12048.
Chandler BM, Lukas S. 2017. Reconstruction of Loch Lomond stadial (Younger Dryas) glaciers on Ben more Coigach, north-west Scotland, and implications for reconstructing palaeoclimate using small ice masses. J Quat Sci. 32(4):475–492. doi:10.1002/jqs.2941.
Chandler BMP, Boston CM, Lukas S. 2019. A spatially-restricted Younger Dryas plateau icefield in the Gaick, Scotland: reconstruction and palaeoclimatic implications. Quat Sci Rev. 211:107–135. doi:10.1016/j.quascirev.2019.03.019.
Chandler BMP, Lovell H, Boston CM, Lukas S, Barr ID, Benediktsson ÍÖ, Benn DI, Clark CD, Darvill CM, Evans DJA, et al. 2018. Glacial geomorphological mapping: a review of approaches and frameworks for best practice. Earth Sci Rev. 185:806–846. doi:10.1016/j.earscirev.2018.07.015.
Enqvist F. 1910. Über die jetzigen und ehemaligen lokalen Gletscher in den Gebirgen von Jämtland und Härjedalen. Die Gletscher Schwedens im Jahre 1908. Sveriges Geol Undersök. 5:1–36.
Evans DJA, Archer S, Wilson DJH. 1999. A comparison of the lichenometric and Schmidt hammer dating techniques based on data from the proglacial areas of some Icelandic glaciers. Quat Sci Rev. 18(1):13–41. doi:10.1016/s0277-3791(98)00098-5.
Evans DJA, Benn D. 2021. Practical guide to the study of glacial sediments. London: Routledge.
Faegri K. 1934. Über die Langenvariationen einiger Gletscher des Jostedalsbre und die dadurch bedingten Pflanzensukzessionen. Bergens Museums Aarbog. 1993:137–142.
Fries C. 1931. Svenska Turistföreningens Årsskrift. Härjedalen: Svenska Turistföreningen.
Furbish DJ, Andrews JT. 1984. The use of hypsometry to indicate long-term stability and response of valley glaciers to changes in mass transfer. J Glaciol. 30(105):199–211. doi:10.3189/S0022143000005931.
Gjerde M, Bakke J, Vasskog K, Nesje A, Hormes A. 2016. Holocene glacier variability and neoglacial hydroclimate at Ålfotbreen, Western Norway. Quat Sci Rev. 133:28–47. doi:10.1016/j.quascirev.2015.12.004.
Gjerde M, Hoel OL, Nesje A. 2023. The 'Little Ice Age' advance of Nigardsbreen, Norway: a cross-disciplinary revision of the chronological framework. Holocene. 33(11):1362–1375. doi:10.1177/09596836231185830.
Glasser NF, Hambrey MJ. 2001. Styles of sedimentation beneath Svalbard valley glaciers under changing dynamic and thermal regimes. J Geol Soc London. 158(4):697–707. doi:10.1144/jgs.158.4.697.
Greenwood SL, Clark CD, Hughes AL. 2007. Formalising an inversion methodology for reconstructing icesheet retreat patterns from meltwater channels: application to the British Ice Sheet. J Quat Sci. 22(6):637–645. doi:10.1002/jqs.1083.
Gunnarson BE, Borgmark A, Wastegård S. 2003. Holocene humidity fluctuations in Sweden inferred from dendrochronology and peat stratigraphy. Boreas. 32(2):347–360. doi:10.1080/03009480310001641.
Haakensen N. 1989. Akkumulasjon på breene i Norge vinteren 1988–89. Været. 3(89):91–94.
Hammarlund D, Velle G, Wolfe BB, Edwards TWD, Barnekow L, Bergman J, Holmgren S, Lamme S, Snowball I, Wohlfarth B, Possnert G. 2004. Palaeolimnological and sedimentary responses to Holocene forest retreat in the Scandes Mountains, west-central Sweden. Holocene. 14(6):862–876. doi:10.1191/0959683604hl756rp.
Hughes ALC, Clark CD, Jordan CJ. 2010. Subglacial bedforms of the last British ice sheet. J Maps. 6(1):543–563. doi:10.4113/jom.2010.1111.

Hughes ALC, Gyllencreutz R, Lohne ØS, Mangerud J, Svendsen JI. 2015. The last Eurasian ice sheets–a chronological database and time-slice reconstruction, DATED-1. Boreas. 45(1):1–45. doi:10.1111/bor.12142.
Humlum O. 1978. Genesis of layered lateral moraines. Geogr Tidsskrift Danish J Geogr. 77(1):65–72. doi:10.1080/00167223.1978.10649094.
Innes JL. 1983. Development of lichenometric dating curves for Highland Scotland. Trans Royal Soc Edinb Earth Sci. 74(1):23–32. doi:10.1017/s0263593300009871.
IPCC. 2023. Summary for policymakers. In: Lee H, Romero J, editor. Climate change 2023: Synthesis report. A report of the intergovernmental panel on climate change. Contribution of working groups I, II and III to the Sixth Assessment Report of the Intergovernmental Panel on Climate Change. Geneva: IPCC; p. 36.
Irvine-Fynn TD, Hodson AJ, Moorman BJ, Vatne G, Hubbard AL. 2011. Polythermal glacier hydrology. A review. Rev Geophys. 49(4):2010R-G000350. doi:10.1029/2010rg000350.
Jansen HL, Simonsen JR, Dahl SO, Bakke J, Nielsen PR. 2016. Holocene glacier and climate fluctuations of the maritime ice cap Høgtuvbreen, northern Norway. Holocene. 26(5):736–755. doi:10.1177/0959683615618265.
Karlén W. 1973. Holocene glacier and climatic variations, Kebnekaise Mountains, Swedish Lapland. Geogr Ann Series A Phys Geogr. 55(1):29–63. doi:10.1080/04353676.1973.11879879.
Karlén W. 1988. Scandinavian glacial and climatic fluctuations during the Holocene. Quat Sci Rev. 7(2):199–209. doi:10.1016/0277-3791(88)90006-6.
Karlén W, Denton G. 1976. Holocene glacial variations in Sarek National Park, northern Sweden. Boreas. 5:25–56. doi:10.1111/j.1502-3885.1976.tb00329.x.
Kjær KH, Krüger J. 2001. The final phase of dead-ice moraine development: processes and sediment architecture, Kötlujökull, Iceland. Sedimentology. 48(5):935–952. doi:10.1046/j.1365-3091.2001.00402.x.
Kleman J, Hättestrand C, Borgström I, Stroeven A. 1997. Fennoscandian palaeoglaciology reconstructed using a glacial geological inversion model. J Glaciol. 43(144):283–299. doi:10.1017/s0022143000003233.
Kleman J, Stroeven AP. 1997. Preglacial surface remnants and quaternary glacial regimes in northwestern Sweden. Geomorphology. 19(1–2):35–54. doi:10.1016/s0169-555x(96)00046-3.
Krog-Larsen N, Knudsen KL, Krohn CF, Kronborg C, Murray AS, Nielsen OB. 2009. Late quaternary ice sheet, Lake and sea history of southwest Scandinavia – a synthesis. Boreas. 38(4):732–761. doi:10.1111/j.1502-3885.2009.00101.x.
Krog-Larsen N, Linge H, Håkansson L, Fabel D. 2012. Investigating the last deglaciation of the Scandinavian ice sheet in southwest Sweden with ^{10}Be exposure dating. J Quat Sci. 27(2):211–220. doi:10.1002/jqs.1536.
Krüger J. 1997. Development of minor outwash fans at Kötlujökull, Iceland. Quat Sci Rev. 16(7):649–659. doi:10.1016/S0277-3791(97)00013-9.
Krüger J, Kjær KH. 1999. A data chart for field description and genetic interpretation of glacial diamicts and associated sediments … with examples from Greenland, Iceland, and Denmark. Boreas. 28(3):386–402. doi:10.1111/j.1502-3885.1999.tb00228.x.
Krüger J, Kjær KH, Van Der Meer JJ. 2002. From push moraine to single-crested dump moraine during a sustained glacier advance. Norsk Geogr Tidssk Norweg J Geogr. 56(2):87–95. doi:10.1080/002919502760056404.
Kuhn M, Markl G, Kaser G, Nickus U, Obleitner F, Schneider H. 1985. Fluctuations of climate and mass balance: different responses of two adjacent glaciers. Zeitsch Gletscherk Glazialgeol. 21(1):409–416.
Kullman L, Kjällgren L. 2000. A coherent postglacial tree-limit chronology (Pinus sylvestris L.) for the Swedish Scandes: aspects of paleoclimate and "Recent warming," based on megafossil evidence. Arct Antarct Alp Res. 32(4):419–428. doi:10.1080/15230430.2000.12003386.
Kullman L, Öberg L. 2020. Shrinking glaciers and ice patches disclose megafossil trees and provide a vision of the Late-glacial and Early post-glacial subalpine/alpine landscape in the Swedish Scandes–review and perspective. J Nat Sci. 8(2):1–15. doi:10.15640/jns.v8n2a1.
Kurop A. 2023. Reconstruction of the glacier dynamics and Holocene chronology of retreat of Helagsglaciären in Central Sweden. Master's thesis no. 660. Lund University, Sweden.
Lacelle D, Lauriol B, Clark ID. 2007. Origin, age, and paleoenvironmental significance of carbonate precipitates from a granitic environment, Akshayuk Pass, southern Baffin Island, Canada. Can J Earth Sci. 44(1):61–79. doi:10.1139/e06-088.
Lantmäteriet. 2022. Geodataportalen. Accessed 3 May 2022. https://www.lantmateriet.se/sv/geodata/Geodataportalen/.
Leigh JR, Stokes CR, Evans DJ, Carr RJ, Andreassen LM. 2020. Timing of Little Ice Age maxima and subsequent glacier retreat in Northern Troms and western Finnmark, Northern Norway. Arct Antarct Alp Res. 52(1):281–311. doi:10.1080/15230430.2020.1765520.
Lie Ø, Dahl SO, Nesje A, Matthews JA, Sandvold S. 2004. Holocene fluctuations of a polythermal glacier in high-alpine eastern Jotunheimen, central-southern Norway. Quat Sci Rev. 23(18-19):1925–1945. doi:10.1016/j.quascirev.2004.03.012.
Linderholm HW. 2005. Summer temperature variability in central Scandinavia during the last 3600 Years. Geogr Ann Series A Phys Geogr. 87(1):231–241. doi:10.1111/j.0435-3676.2005.00255.x.

Lipovsky BP, Meyer CR, Zoet LK, McCarthy C, Hansen DD, Rempel AW, Gimbert F. 2019. Glacier sliding, seismicity and sediment entrainment. Ann Glaciol. 60(79):182–192. doi:10.1017/aog.2019.24.
Lukas S. 2005. A test of the englacial thrusting hypothesis of 'hummocky' moraine formation: case studies from the northwest Highlands, Scotland. Boreas. 34(3):287–307. doi:10.1111/j.1502-3885.2005.tb01102.x.
Lukas S. 2007. Early-Holocene glacier fluctuations in Krundalen, south central Norway: palaeo-glacier dynamics and palaeoclimate. Holocene. 17(5):585–598. doi:10.1177/095968360707898.
Lukas S. 2011. Ice-cored moraines. In: Singh VP, Singh P, Haritashya UK, editor. Encyclopedia of snow, ice and glaciers. Dordrecht: Springer; p. 616–619.
Lukas S, Bradwell T. 2010. Reconstruction of a late-glacial (Younger Dryas) mountain ice field in Sutherland, northwestern Scotland, and its palaeoclimatic implications. J Quat Sci. 25(4):567–580. doi:10.1002/jqs.1376.
Lukas S, Graf A, Coray S, Schlüchter C. 2012. Genesis, stability and preservation potential of large lateral moraines of alpine valley glaciers – towards a unifying theory based on Findelengletscher, Switzerland. Quat Sci Rev. 38:27–48. doi:10.1016/j.quascirev.2012.01.022.
Lundqvist J. 1969. Beskrivning till Jordartskarta över Jämtlands län. Sveriges geologiska undersökning Ca 45. Sweden.
Mallinson L, Swift DA, Sole A. 2019. Proglacial icings as indicators of glacier thermal regime: ice thickness changes and icing occurrence in Svalbard. Geogr Ann Series A Phys Geogr. 101(4):334–349. doi:10.1080/04353676.2019.1670952.
Matthews JA. 2005. Little Ice Age' glacier variations in Jotunheimen, southern Norway: a study in regionally controlled lichenometric dating of recessional moraines with implications for climate and lichen growth rates. Holocene. 15(1):1–19. doi:10.1191/0959683605hl779rp.
Matthews JA, Dresser PQ. 2008. Holocene glacier variation chronology of the Smørstabbtindan massif, Jotunheimen, southern Norway, and the recognition of century-to millennial-scale European Neoglacial events. Holocene. 18(1):181–201. doi:10.1177/0959683607085608.
Mooers HD. 1990. A glacial-process model: the role of spatial and temporal variations in glacier thermal regime. Geol Soc Am Bull. 102(2):243–251. doi:10.1130/0016-7606(1990)102<0243:agpmtr>2.3.co;2.
Nesje A. 2009. Latest Pleistocene and Holocene alpine glacier fluctuations in Scandinavia. Quat Sci Rev. 28(21–22):2119–2136. doi:10.1016/j.quascirev.2008.12.016.
Nesje A, Dahl SO, Thun T, Nordli Ø. 2007. The 'Little Ice Age' glacial expansion in western Scandinavia: summer temperature or winter precipitation? Clim Dyn. 30(7–8):789–801. doi:10.1007/s00382-007-0324-z.
Nesje A, Lie Ø, Dahl SO. 2000. Is the North Atlantic oscillation reflected in Scandinavian glacier mass balance records? J Quat Sci. 15(6):587–601. doi:10.1002/1099-1417(200009)15:6<587::aid-jqs533>3.0.co;2-2.
Norris SL, Margold M, Froese DG. 2017. Glacial landforms of Northwest Saskatchewan. J Maps. 13(2):600–607. doi:10.1080/17445647.2017.1342212.
Öberg L, Kullman L. 2011. Recent glacier recession: a new source of postglacial treeline and climate history in the Swedish Scandes. Landsc Online. 26(1):1–38. doi:10.3097/LO.201126.
Ohmura A, Kasser P, Funk M. 1992. Climate at the equilibrium line of glaciers. J Glaciol. 38(130):397–411. doi:10.3189/s0022143000002276.
Oien RP, Rea BR, Spagnolo M, Bingham RG. 2022. Testing the area–altitude balance ratio (AABR) and accumulation–area ratio (AAR) methods of calculating glacier equilibrium-line altitudes. J Glaciol. 68(268):357–368. doi:10.1017/jog.2021.100.
Olsen J, Anderson NJ, Knudsen MF. 2012. Variability of the North Atlantic oscillation over the past 5,200 years. Nat Geosci. 5(11):808–812. doi:10.1038/ngeo1589.
O'Neal MA. 2006. The effects of slope degradation on lichenometric dating of Little Ice Age moraines. Quat Geochronol. 1(2):121–128. doi:10.1016/j.quageo.2006.05.025.
OPENGIS.ch. 2022. QField: the most powerful and efficient way to manage your data on-the-go. Accessed 5 June 2022. https://qfield.org/.
Osborn G, McCarthy D, LaBrie A, Burke R. 2015. Lichenometric dating: science or pseudo-science? Quat Res. 83(1):1–12. doi:10.1016/j.yqres.2014.09.006.
Osmaston HA. 2005. Estimates of glacier equilibrium line altitudes by the area×altitude, the area×altitude balance ratio and the area×altitude balance index methods and their validation. Quat Int. 138–139:22–31. doi:10.1016/j.quaint.2005.02.004.
Osmaston HA. 2006. Should quaternary sea-level changes be used to correct glacier ELAs, vegetation belt altitudes and sea level temperatures for inferring climate changes? Quat Res. 65(2):244–251. doi:10.1016/j.yqres.2005.11.004.
Pellitero R, Rea BR, Spagnolo M, Bakke J, Hughes P, Ivy-Ochs S, Lukas S, Ribolini A. 2015. A GIS tool for automatic calculation of glacier equilibrium-line altitudes. Comput Geosci. 82:55–62. doi:10.1016/j.cageo.2015.05.005.
Pellitero R, Rea BR, Spagnolo M, Bakke J, Ivy-Ochs S, Frew CR, Hughes P, Ribolini A, Lukas S, Renssen H. 2016. GlaRe, a GIS tool to reconstruct the 3D surface of palaeoglaciers. Comput Geosci. 94:77–85. doi:10.1016/j.cageo.2016.06.008.

Radić V, Hock R. 2006. Modelling future glacier mass balance and volume changes using ERA-40 reanalysis and climate models: A sensitivity study at Storglaciären, Sweden. J Geophys Res Earth Surf. 111:F3. doi:10.1029/2005jf000440.

Rea BR. 2009. Defining modern day area-altitude balance ratios (AABRs) and their use in glacier-climate reconstructions. Quat Sci Rev. 28(3–4):237–248. doi:10.1016/j.quascirev.2008.10.011.

Rea BR, Pellitero R, Spagnolo M, Hughes P, Ivy-Ochs S, Renssen H, Ribolini A, Bakke J, Lukas S, Braithwaite RJ. 2020. Atmospheric circulation over Europe during the younger Dryas. Sci Adv. 6(50):eaba4844. doi:10.1126/sciadv.aba4844.

Regnéll C. 2016. Holocene glacier extents and equilibrium-line altitude (ELA) reconstructions of paleoglaciers in Sarek National Park, northern Sweden. Master thesis no B905 at University of Gothenburg.

Rehn I. 2019. Mass balance and local characteristics of three glaciers in southern Norway, between 1980 and 2018. An analysis of the mass balance and the local characteristics of Ålfotbreen, Storbreen and Gråsubreen. Bachelor's thesis no. GG 242, Stockholm University, Sweden. doi:10.13140/RG.2.2.17396.17282/1.

Reinardy BT, Booth AD, Hughes AL, Boston CM, Åkesson H, Bakke J, Nesje A, Giesen RH, Pearce DM. 2019. Pervasive cold ice within a temperate glacier – implications for glacier thermal regimes, sediment transport and foreland geomorphology. Cryosphere. 13(3):827–843. doi:10.5194/tc-13-827-2019.

Reinardy BT, Leighton I, Marx PJ. 2013. Glacier thermal regime linked to processes of annual moraine formation at Midtdalsbreen, Southern Norway. Boreas. 42(4):896–911. doi:10.1111/bor.12008.

Rettig L, Lukas S, Huss M. 2023. Implications of a rapidly thinning ice margin for annual Moraine Formation at Gornergletscher, Switzerland. Quat Sci Rev. 308:108085. doi:10.1016/j.quascirev.2023.108085.

Rosqvist GC, Jonsson C, Yam R, Karlén W, Shemesh A. 2004. Diatom oxygen isotopes in pro-glacial lake sediments from northern Sweden: a 5000 year record of atmospheric circulation. Quat Sci Rev. 23(7–8):851–859. doi:10.1016/j.quascirev.2003.06.009.

Rosqvist GC, Leng MJ, Goslar T, Sloane HJ, Bigler C, Cunningham L, Dadal A, Bergman J, Berntsson A, Jonsson C, Wastegård S. 2013. Shifts in precipitation during the last millennium in northern Scandinavia from Lacustrine Isotope Records. Quat Sci Rev. 66:22–34. doi:10.1016/j.quascirev.2012.10.030.

Seier G, Abermann J, Andreassen LM, Carrivick JL, Kielland PH, Löffler K, Yde JC. 2024. Glacier thinning, recession and advance, and the associated evolution of a glacial lake between 1966 and 2021 at Austerdalsbreen, western Norway. Land Degrad Dev. 35(1):394–414.

Seppä H, Hammarlund D and Antonsson K. 2005. Low-frequency and high-frequency changes in temperature and effective humidity during the Holocene in south-central Sweden: implications for atmospheric and oceanic forcings of climate. Clim Dyn 25(2–3): 285–297. https://doi.org/10.1007/s00382-005-0024-5

[SGU] Sveriges Geologiska Undersökning. 2017. Berggrund geologi. Kartvisare. Accessed 5 May 2022. https://apps.sgu.se/kartvisare/kartvisare-berg-50-250-tusen.html.

[SGU] Sveriges Geologiska Undersökning. 2021. Jordarter 1:25 000–1:100 000. Kartvisare. Accessed 5 May 2022. https://apps.sgu.se/kartvisare/kartvisare-jordarter-25-100.html.

[SMHI] Sveriges Meteorologiska och Hydrologiska Institut. 2013. Nederbörd. Accessed 11 July 2022. https://www.smhi.se/kunskapsbanken/meteorologi/nederbord/nederbord-1.361.

Snowball I, Muscheler R, Zillén L, Sandgren P, Stanton T, Ljung K. 2010. Radiocarbon wiggle matching of Swedish lake varves reveals asynchronous climate changes around the 8.2 Kyr cold event. Boreas. 39(4):720–733. doi:10.1111/j.1502-3885.2010.00167.x.

Snowball I, Zillén L, Gaillard MJ. 2002. Rapid early-Holocene environmental changes in northern Sweden based on studies of two varved lake-sediment sequences. Holocene. 12(1):7–16. doi:10.1191/0959683602hl515rp.

Stroeven AP, Hättestrand C, Kleman J, Heyman J, Fabel D, Fredin O, Goodfellow BW, Harbor JM, Jansen JD, Olsen L, et al. 2016. Deglaciation of Fennoscandia. Quat Sci Rev. 147:91–121. doi:10.1016/j.quascirev.2015.09.016.

Sundqvist HS, Holmgren K, Lauritzen SE. 2007. Stable isotope variations in stalagmites from northwestern Sweden document climate and environmental changes during the early Holocene. Holocene. 17(2):259–267. doi:10.1177/0959683607073292.

Sutherland JL, Carrivick JL, Gandy N, Shulmeister J, Quincey DJ, Cornford SL. 2020. Proglacial lakes control glacier geometry and behavior during recession. Geophys Res Lett. 47(19):e2020GL088865. doi:10.1029/2020GL088865.

Svendsen JI, Alexanderson H, Astakhov VI, Demidov I, Dowdeswell JA, Funder S, Gataullin V, Henriksen M, Hjort C, Houmark-Nielsen M, et al. 2004. Late quaternary ice sheet history of Northern Eurasia. Quat Sci Rev. 23(11–13):1229–1271. doi:10.1016/j.quascirev.2003.12.008.

Syverson KM, Mickelson DM. 2009. Origin and significance of lateral meltwater channels formed along a temperate glacier margin, Glacier Bay, Alaska. Boreas. 38(1):132–145. doi:10.1111/j.1502-3885.2008.00042.x.

Taveirne M, Ekemar L, González Sánchez B, Axelsson J, Zhang Q. 2021. Mass balance sensitivity and future projections of Rabots Glaciär, Sweden. Climate. 9(8):126. doi:10.3390/cli9080126.

Terleth Y, van Pelt WJJ, Pettersson R. 2022. Spatial variability in winter mass balance on Storglaciären modelled with a terrain-based approach. J Glaciol. 69(276):749–761. doi:10.1017/jog.2022.96.

Tinnerholm H. 2024. Mapping and Modeling the Retreat of the Helags Cirque Glacier in Härjedalen, Sweden. Master thesis at University of Gothenburg. https://hdl.handle.net/2077/81738.

Tonkin TN, Midgley NG, Labadz JC. 2016. Internal structure and significance of ice-marginal moraine in the Kebnekaise Mountains, northern Sweden. Boreas. 46(2):199–211. doi:10.1111/bor.12220.
Valladares F, Sancho LG. 1995. Lichen colonization and recolonization of two recently deglaciated zones in the maritime Antarctic. Lichenologist. 27(6):485–493. doi:10.1016/S0024-2829(95)80008-5.
Velle G, Brooks SJ, Birks HJB, Willassen E. 2005. Chironomids as a tool for inferring Holocene climate: an assessment based on six sites in southern Scandinavia. Quat Sci Rev. 24(12–13):1429–1462. doi:10.1016/j.quascirev.2004.10.010.
Wastegård S. 2022. The Holocene of Sweden – a review. GFF. 144(2):126–149. doi:10.1080/11035897.2022.2086290.
[WGMS] World Glacier Monitoring Service. 2021. Data exploration. Accessed 15 July 2022. https://wgms.ch/data-exploration/.
Winchester V, Harrison S. 2000. Dendrochronology and lichenometry: colonization, growth rates and dating of geomorphological events on the east side of the North Patagonian Icefield, Chile. Geomorphology. 34(3-4):181–194. doi:10.1016/S0169-555X(00)00006-4.
Winkler S. 2004. Lichenometric dating of the 'Little Ice Age' maximum in Mt Cook National Park, Southern Alps, New Zealand. Holocene. 14(6):911–920. doi:10.1191/0959683604hl767rp.
Wyshnytzky CE, Lukas S, Groves JWE. 2021. Multiple mechanisms of minor moraine formation in the Schwarzensteinkees Foreland, Austria. In: Waitt RB, Thackray GD, Gillespie AR untangling the quaternary period – a legacy of Stephen C. Porter. The Geological Society of America 548. doi:10.1130/2020.2548(10).
Zhang P, Linderholm HW, Gunnarson BE, Björklund J, Chen D. 2016. 1200 years of warm-season temperature variability in central Scandinavia inferred from tree-ring density. Clim Past. 12(6):1297–1312. doi:10.5194/cp-12-1297-2016.